

August 2022

**Name & Qualifications**

Associate Professor Marnie Forster

**Department / School / Centre**

College of Science  
Research School of Earth Sciences  
Argon Facility  
**+61 425603412**  
Marnie.forster@anu.edu.au

Canberra ACT 0200 Australia  
**www.anu.edu.au**

CRICOS Provider No. 00120C

ANU Argon Facility Technical Report: ANU15-2021

**$^{40}\text{Ar}/^{39}\text{Ar}$  Analysis**

**For NATIONAL ARGON MAP**

**By Marnie Forster and Davood Vasegh**

NAM PROJECT 22:

TITLE:

**Ar/Ar thermochronology age constraints on mafic  
and felsic magmatism, and deformation in the  
Curnamona Province**

(The basalt samples are analysed by Melbourne Uni Argon Lab)



This project was enabled by NCRIS via AuScope



This work has been undertaken to support MinEx CRC

<b>Sample Provider</b>	Chris Folkes (Geological Survey of New South Wales)
<b>Financial Contributor</b>	Argon Analysis: Geoscience Australia Mineral Separation: GA Mineral Separation: GSSA
<b>Mineral Separation</b>	Mineral Separation Facility at Research School of Earth Sciences, ANU
<b>Analysis Methodology &amp; Interpretation</b>	Marnie Forster at ANU Argon Facility
<b>Sample Analysis</b>	Davood Vasegh at ANU Argon Facility
<b>Data Reduction</b>	Davood Vasegh at ANU Argon Facility
<b>Supplementary Information</b>	Marnie Forster and Davood Vasegh at ANU Argon Facility

## Proposal 22:

# **Ar/Ar thermochronology age constraints on mafic and felsic magmatism, and deformation in the Curnamona Province**

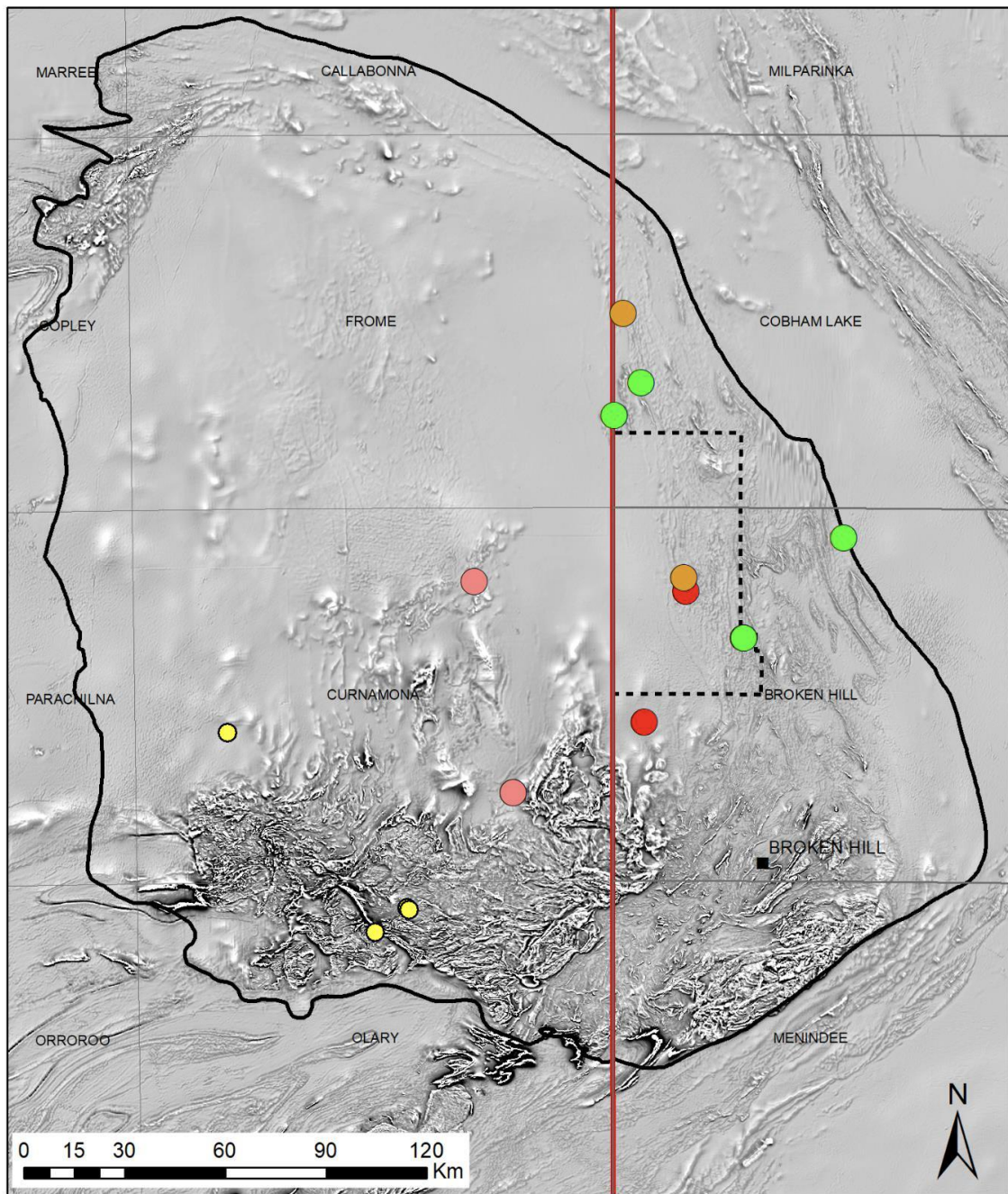
Geographic Region: Mundi Mundi Plain, Olary Domain

Geological Province: Curnamona Province

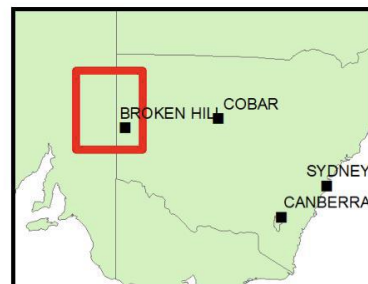
The Mundi NDI area in NSW contains outcrop and drillholes that have intersected numerous metasedimentary rocks (e.g. schist, slate) interpreted to belong to Paleoproterozoic basement units (i.e. the Paragon Group - Willyama Supergroup). The rock units show strong deformation fabrics with the growth of micaceous minerals that would be good targets to date using Ar/Ar methods. Some samples have been collected from outcrop and legacy drillcore). There are few pre-existing geochronological dates/constraints on the proposed samples. If these samples are indeed from Willyama Supergroup basement rocks, then this would suggest the main deformation age would be the Olarian Orogeny at 1600-1580 Ma. The Ar/Ar analysis of Mundi Mundi Granite would help in constructing the thermal history of the Curnamona province

The Mundi NDI area in NSW contains numerous mapped instances of mafic volcanic and intrusive rocks. These are mostly undercover and intersected by a handful of drillholes throughout the region. The main formal stratigraphic unit these have been assigned to is the Wilangee Basalt (NSW Seamless Geology; Colquhoun et al. 2020). Little geochemical analyses and no geochronological data have been completed for mafic rocks assigned.

The main aim in submitting the basaltic rocks for geochronological analysis is to determine their associated tectono-magmatic event. Possibilities include: the break-up of the Rodinian Supercontinent (different pulses of Neoproterozoic Adelaidean rifting) from ~830-540 Ma; volcanic-arc magmatism associated with the Delamerian Cycle from ~540-510 Ma; or another unknown magmatic event.



- SA samples - Reid**
- Previous NAM samples
  - This proposal (granitoids)
- NSW samples - Folkes**
- Basalt
  - Granite
  - Schist/metaseds
- 250K standard map areas  
 □ NSW-SA border  
 □ Mundi NDI area  
 □ GA Provinces Curnamona Province  
 ■ Large Towns



*Location Figure: Location of proposed samples from the Curnamona Province. The MinEx CRC Mundi NDI area is shown. The background image shows the 2019 Geoscience Australia greyscale national total magnetic image (TMI) first vertical derivative (1VD). Previous samples submitted for the National Argon Map from the Curnamona Province in South Australia are also shown*

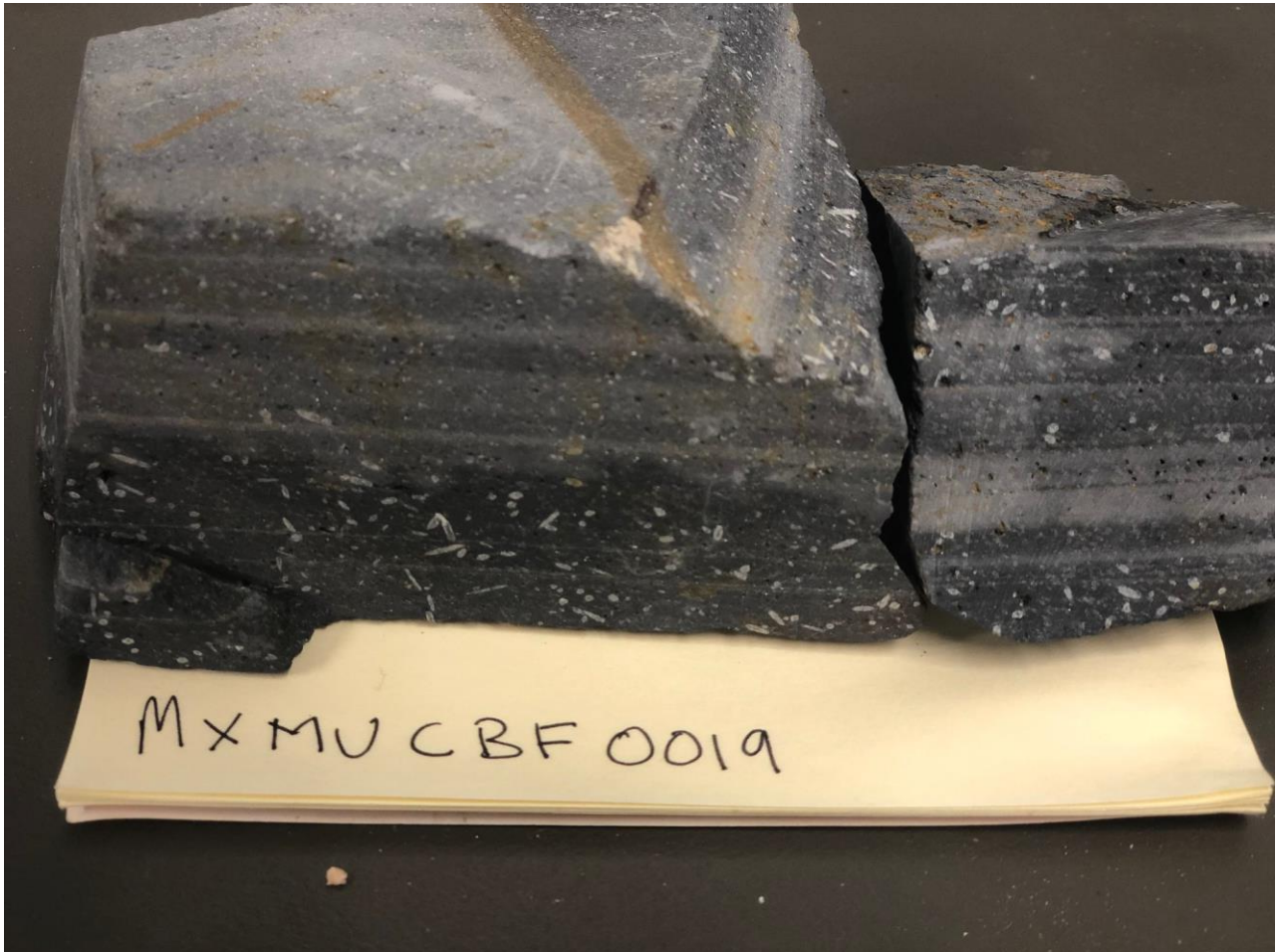
## Sample information from proposal and locations:

ANU CAN	Target Mineral	Identification No.	Foil No.	Mass mg	Survey and Researcher
CAN #38	Micas	MXMUCBF0019	A1	3.1	GSNSW - Folkes
CAN #38	Micas	MXMUCBF0006	A2	2.4	GSNSW - Folkes
CAN #38	Hornblende	3704279	A3	83.6	GSSA - Reid
CAN #38	Biotite	3704279	A4	3.7	GSSA - Reid
CAN #38	Muscovite	2876974	A5	3.5	GSSA - Reid
CAN #38 then CAN #39	K-feldspar	2876974	A6/Z6	4.4	GSSA - Reid
CAN #35	White mica	Mundi Granite MXMUCBF0001.01E	N15	3.5	GSNSW – Yates/Folkes
CAN #35	K-feldspar	Mundi Granite MXMUCBF0001.01E	N16	4.2	GSNSW – Yates/Folkes
CAN #35	Biotite	Mundi Granite MXMUCBF0001.01E	N17	3.6	GSNSW – Yates/Folkes

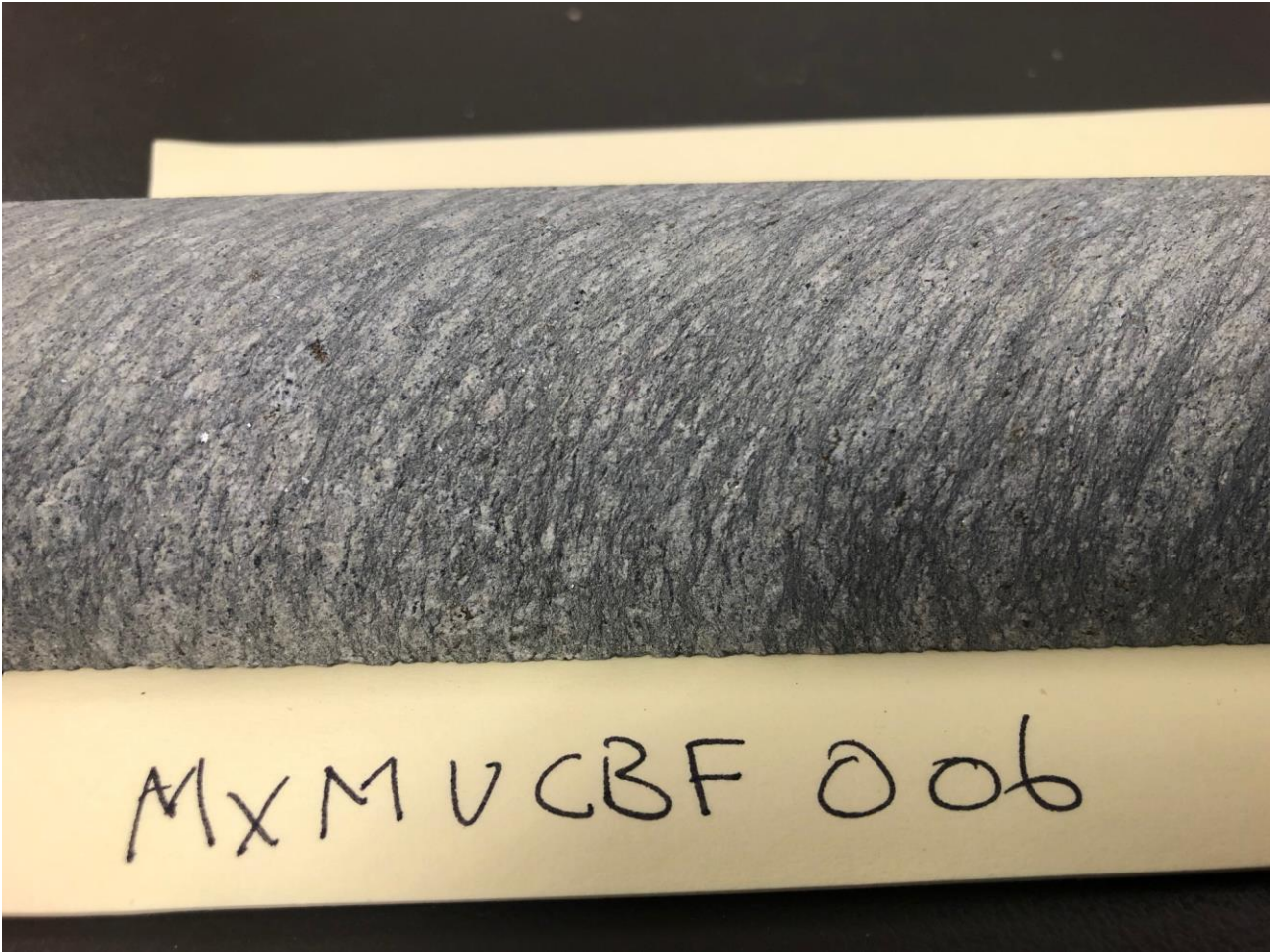
**Note:** A6 was unsuccessful due to a mass spectrometer problem and was analysed again as Z6

# Sample Description and Rock Photograph

**Sample MXMUCBF0019:** Separated for micas



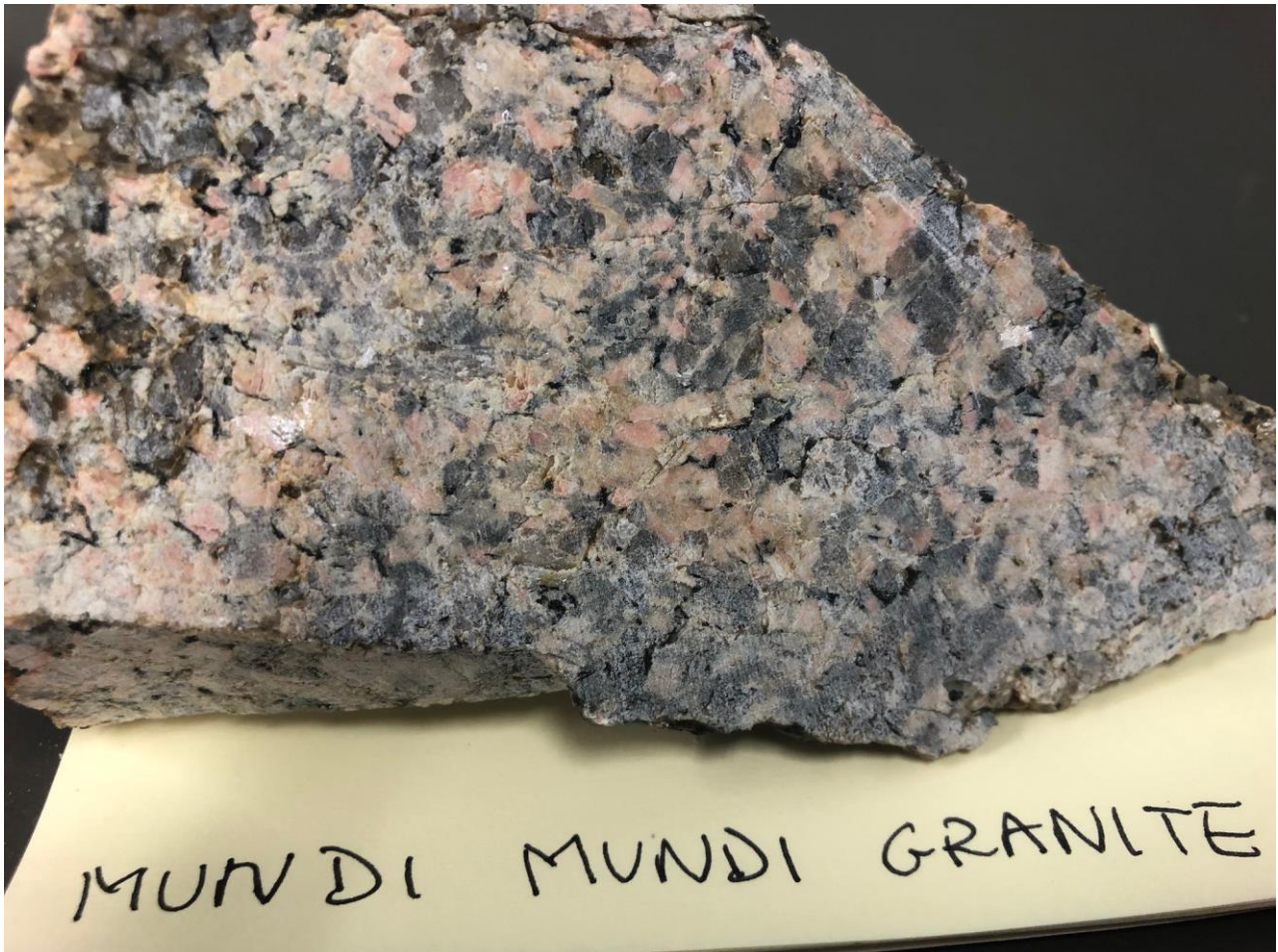
**Sample MXMUCBF0006:** Separated for micas



**No Rock photographs available for Sample Number 2704279 or 2876974.**

**Sample for Mundi Mundi Granite MXMCBF0001.01E:** Separated for K-feldspar, white mica and biotite.

Cambro-Ordovician magmatism and deformation at the eastern margin of Gondwana, South Australia: Insights into tectonic processes and mineral potential. The sample was collected near Boulder tank area - Location: WGS85 Latitude  $31^{\circ}13'26.00''\text{S}$ , longitude  $141^{\circ}13'43.00''\text{E}$  on Broken Hill Map.



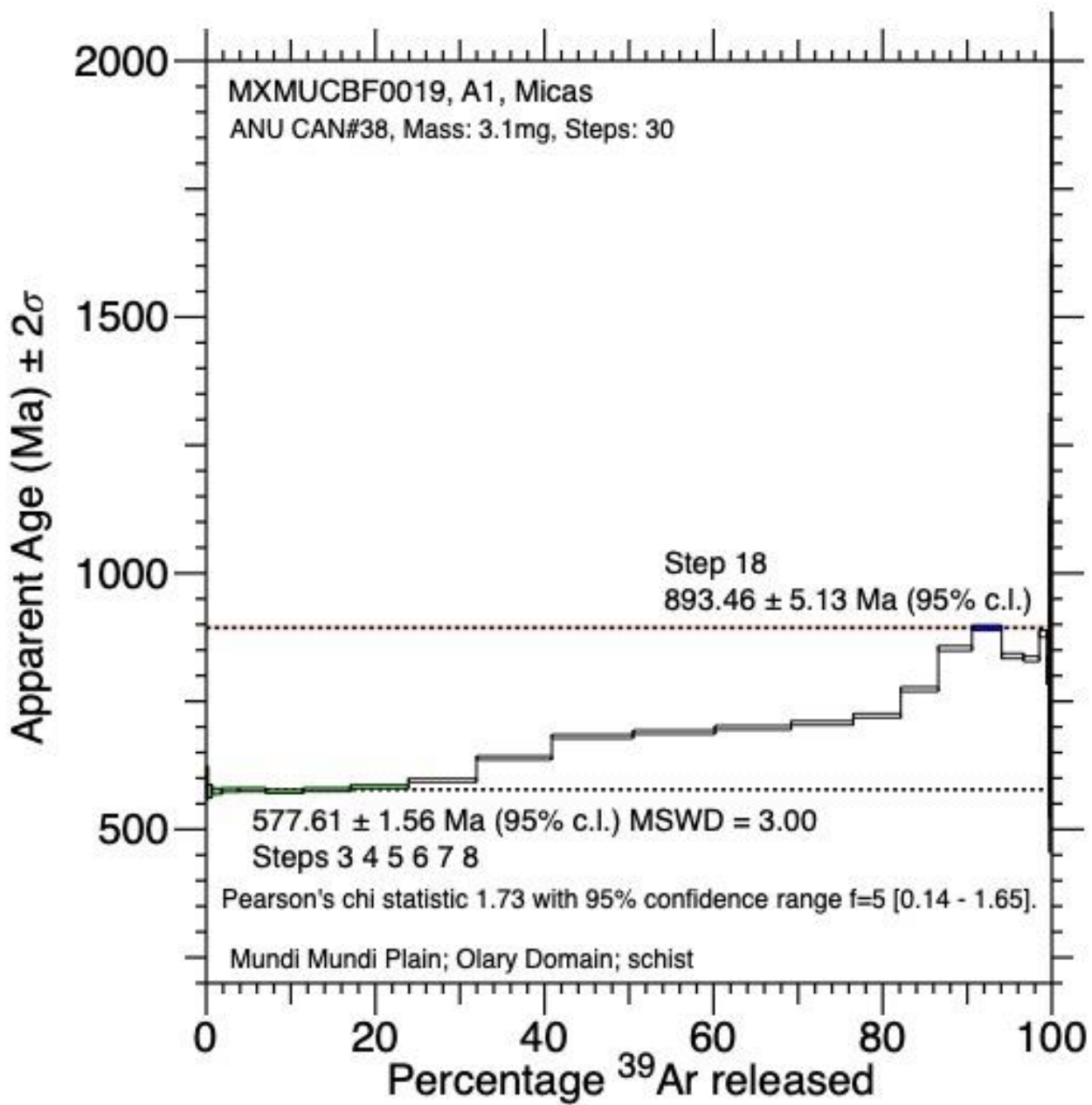


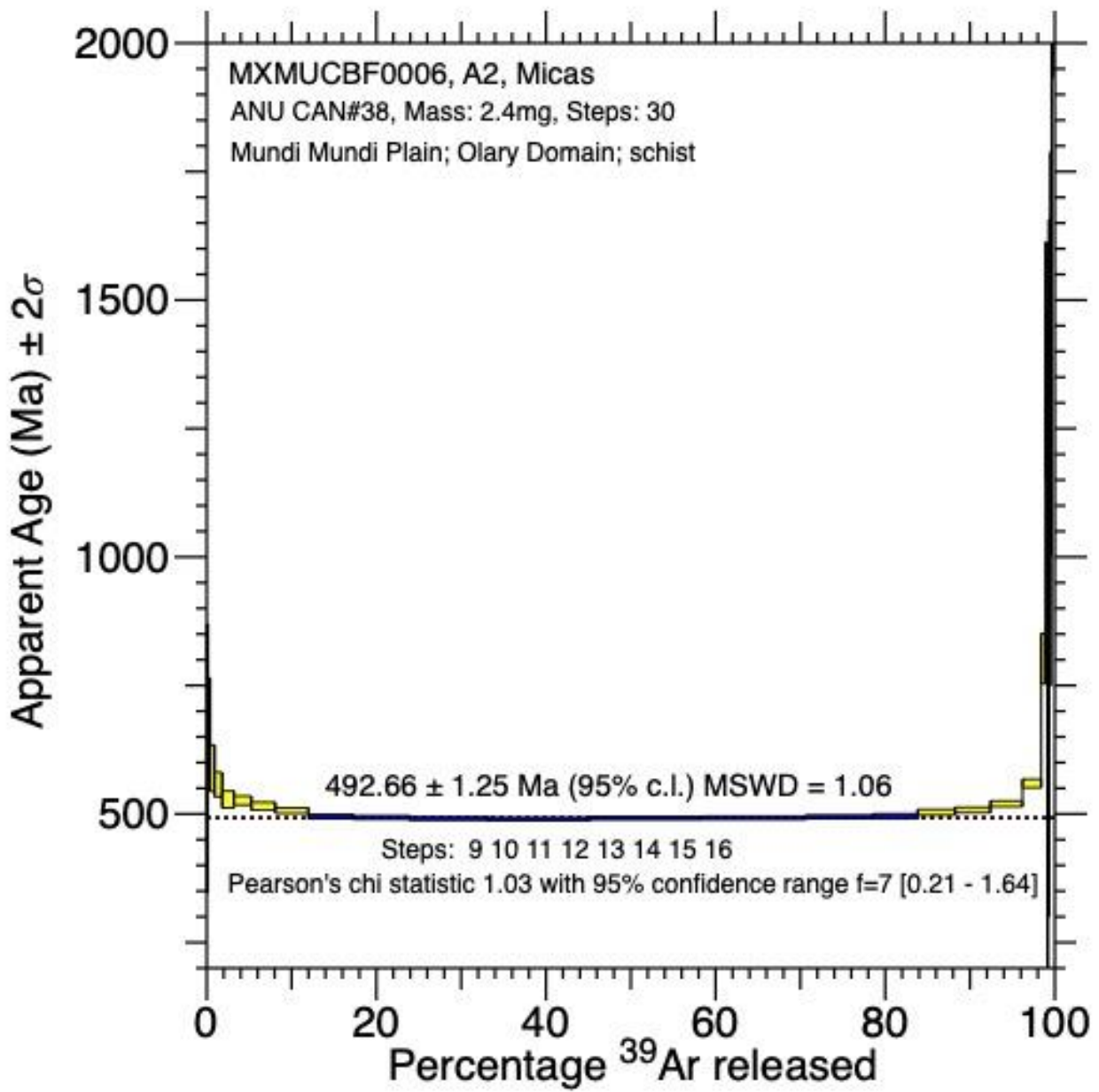
## $^{40}\text{Ar}/^{39}\text{Ar}$ analysis plots and information

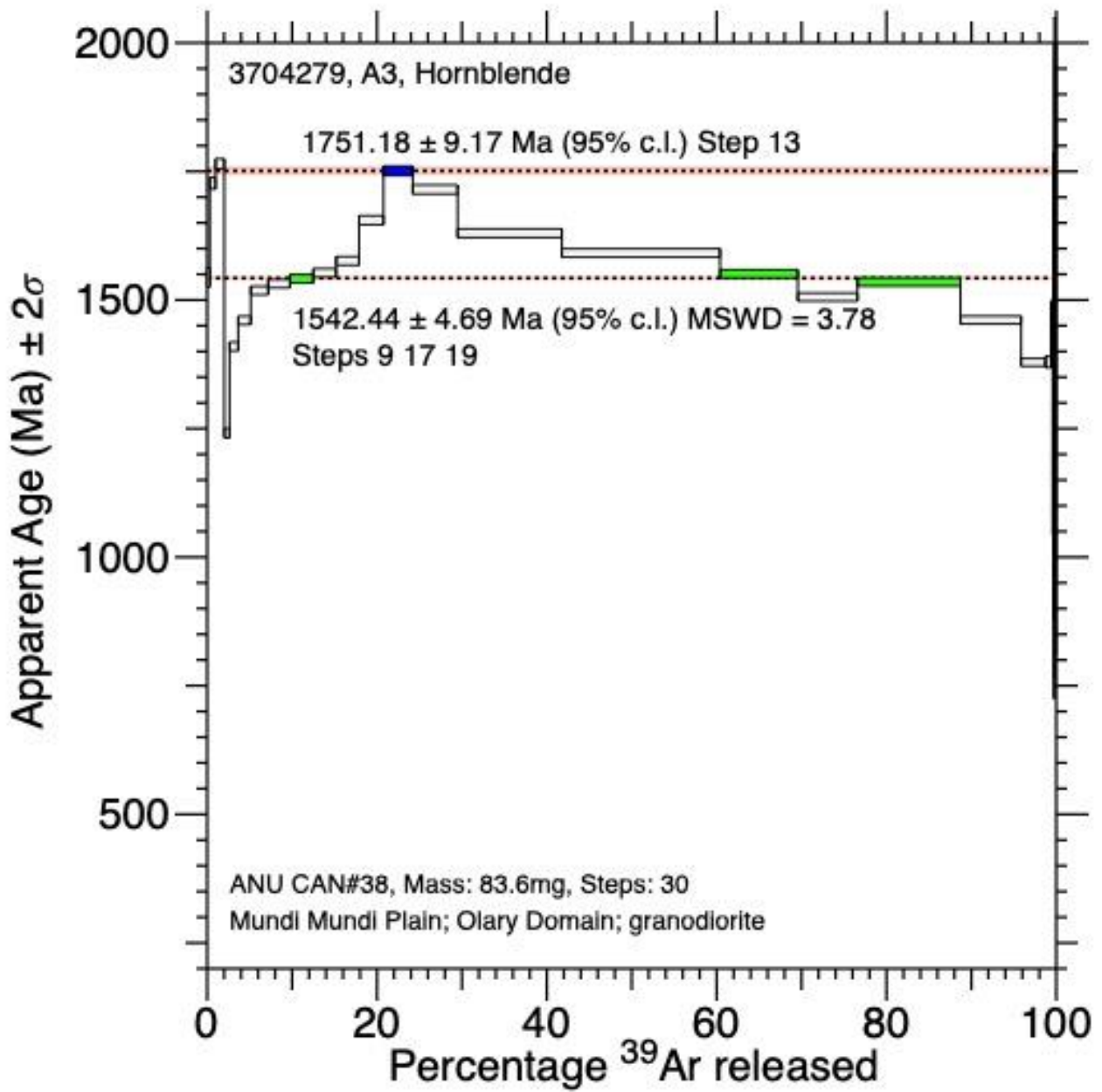
The age plots are interpreted using the Asymptote and Limits method (Forster and Lister 2004). The argon system is affected by heat, for example if a sample is heated long enough then the argon system will be completely reset, if however, it is heated for a relatively short period of time and/or with temperatures that are not extreme then the sample may be only partially reset. Thus, relic ages can be retained and likewise overprinting events can be recorded and not overprint the argon system completely. As a consequence, the argon plots can have more than one 'age'. In many cases a minor overprinting event can be seen in these plots, it will be a maximum age and not necessary an accurate age but does show that a younger overprinting event did occur. It can be seen in the age plots that after the steps that record the youngest event, they are followed by diffusional loss and/or mixing towards the older ages that are highlighted in blue or green.

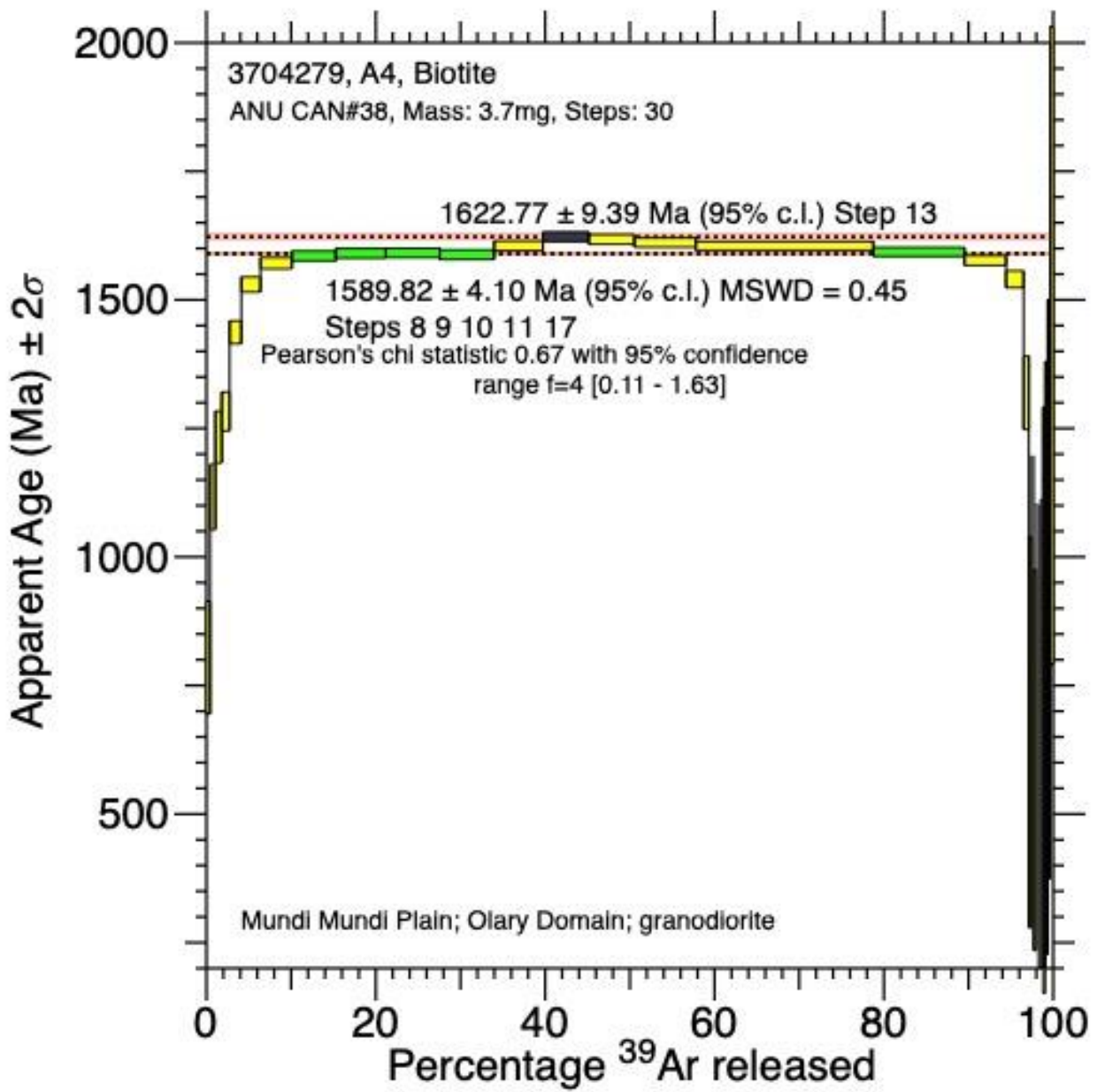
The argon data results are presented as Apparent Age Plots. The age data is presented on these plots showing the ages for different populations within each sample. Each age is highlighted and has a dashed orange line defined and shows the error, the MSWD, the steps representing the % gas release, and the Pearsons chi statistics for each of these domains is presented where applicable. There can be multiple ages defined on each spectrum: which represent different age gas populations/reservoirs. In addition, there is the sample identification number; the foil number; the mineral; the ANU canister number; the mass used and the number of steps. At the base of the plot is the sample information e.g. location.

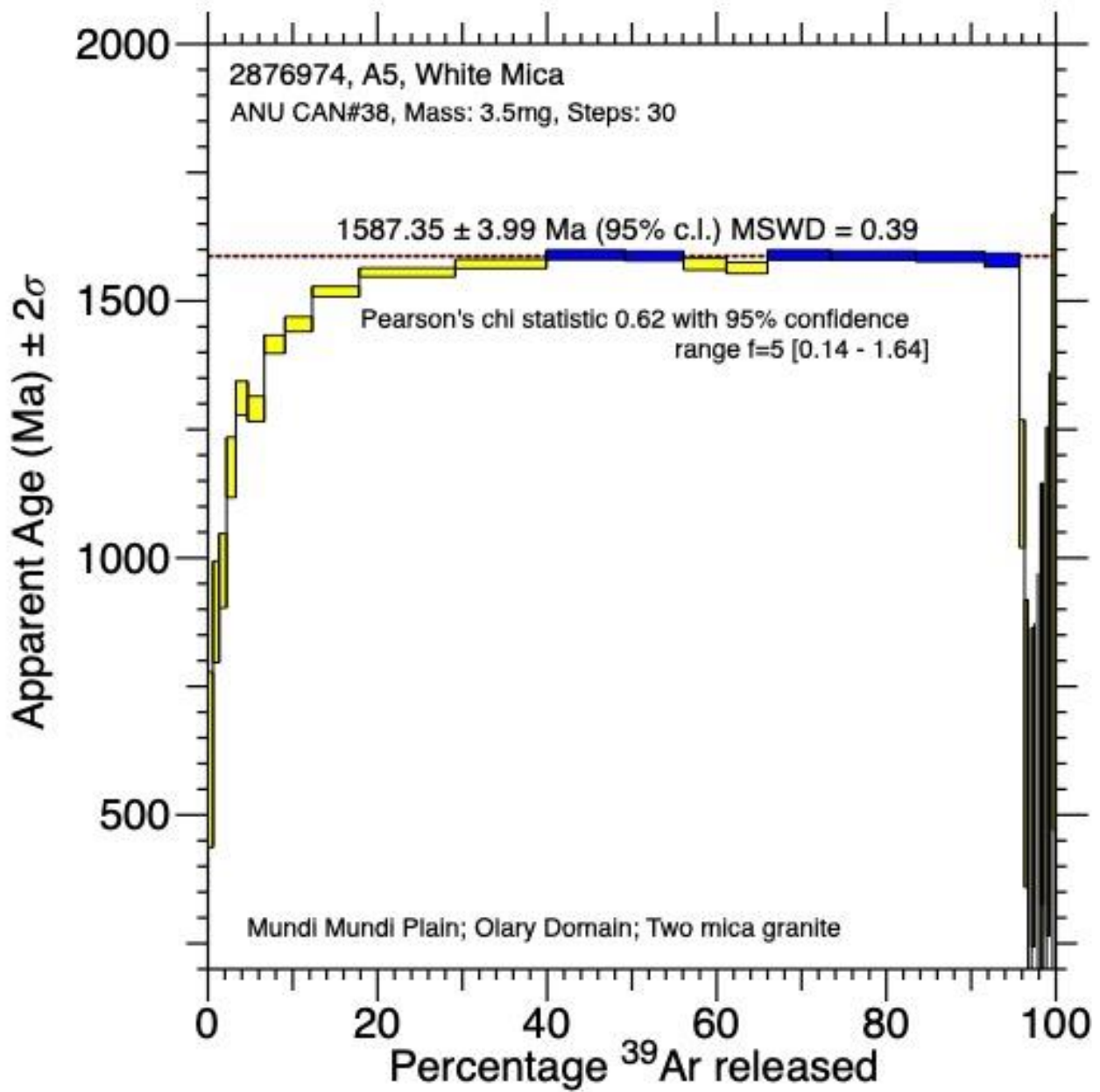
*Summary:* Each of the selected interpreted ages have been labelled with a dashed orange line and the age and age data placed on that line. This includes the age, the calculated error, the MSWD and all to 95% c.i. These blue or green highlighted selected steps represent an age population. Note that in several cases the mixing steps are yellow (this is a software aspect and is meaningless).

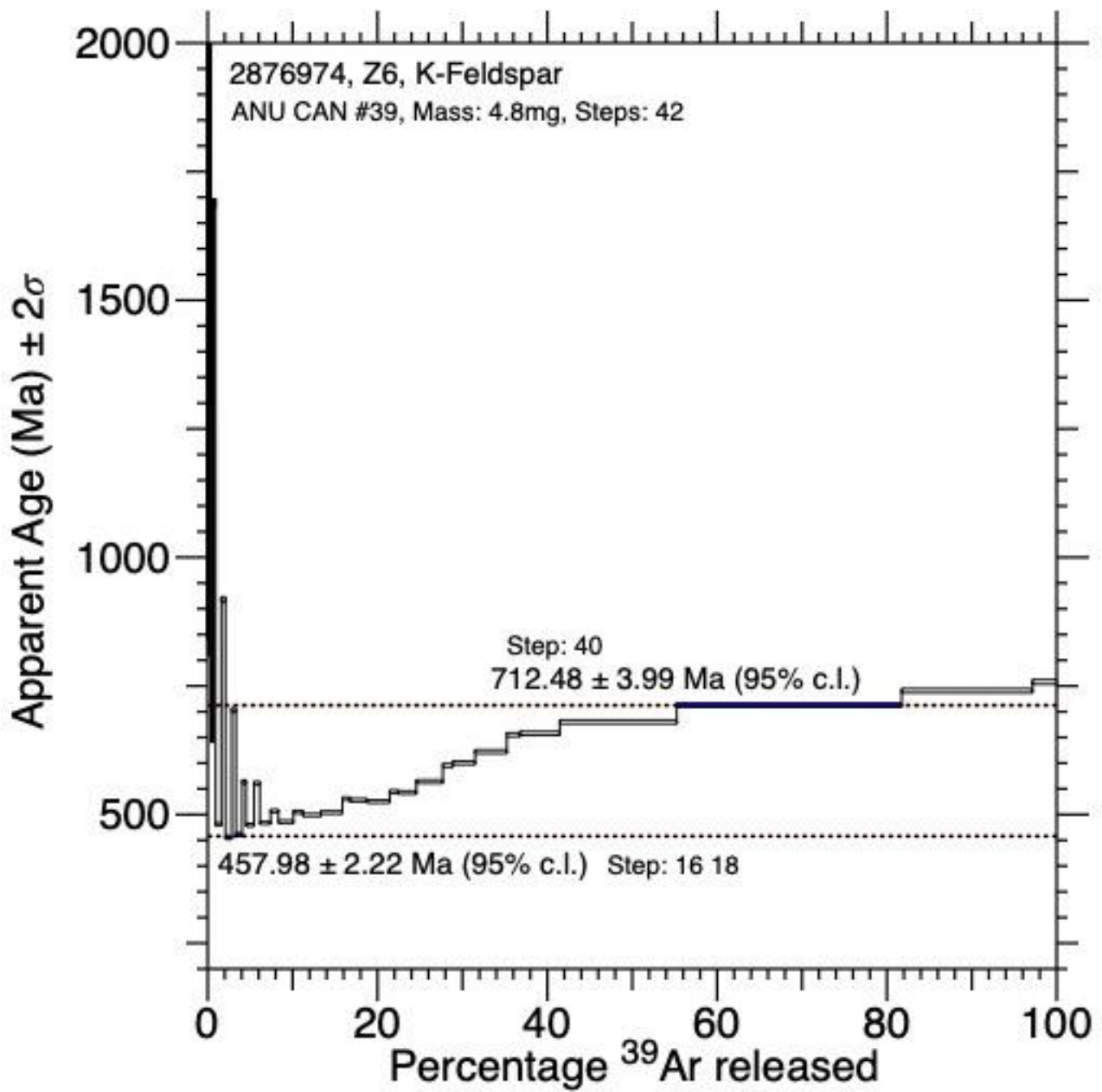


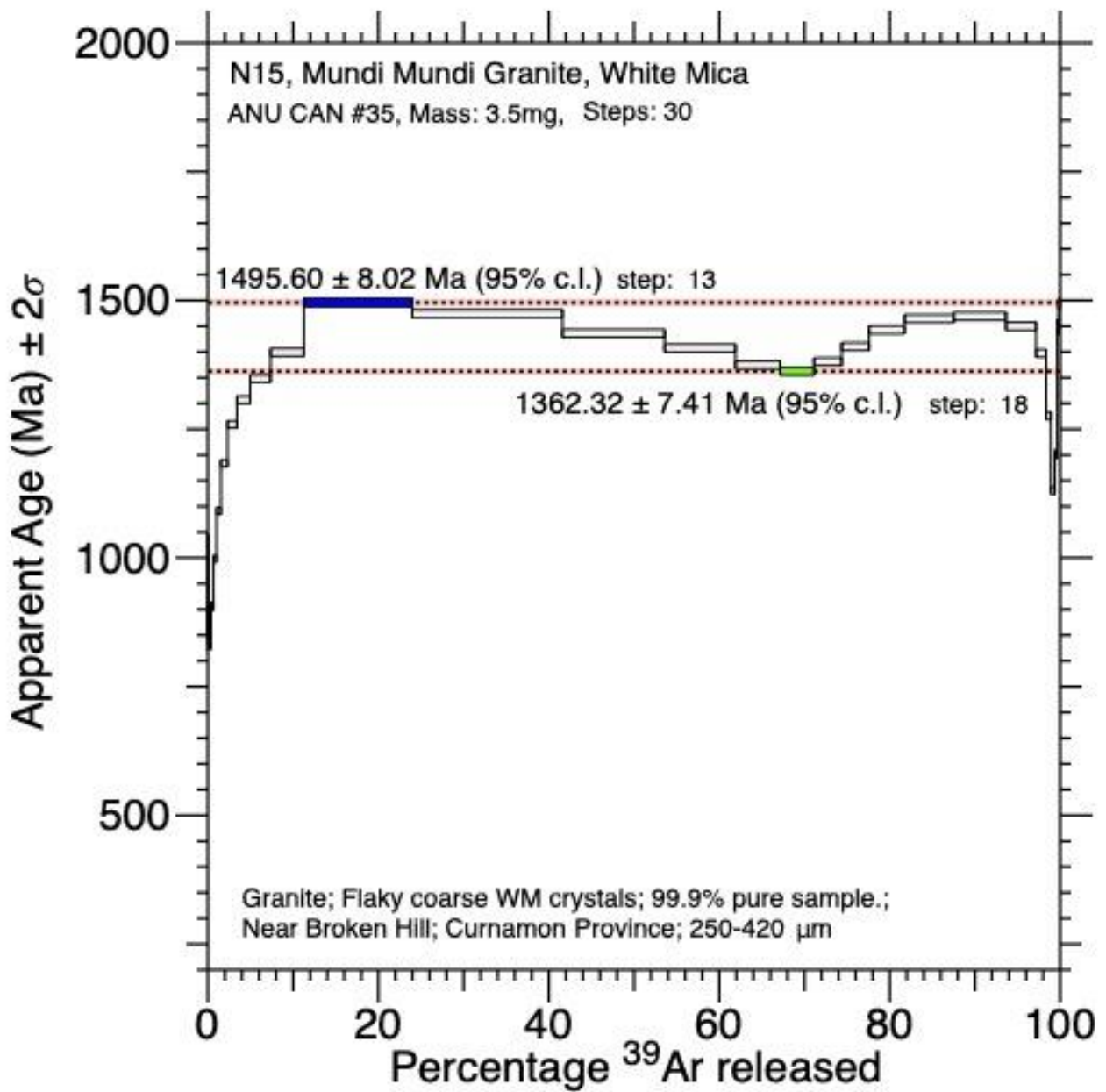




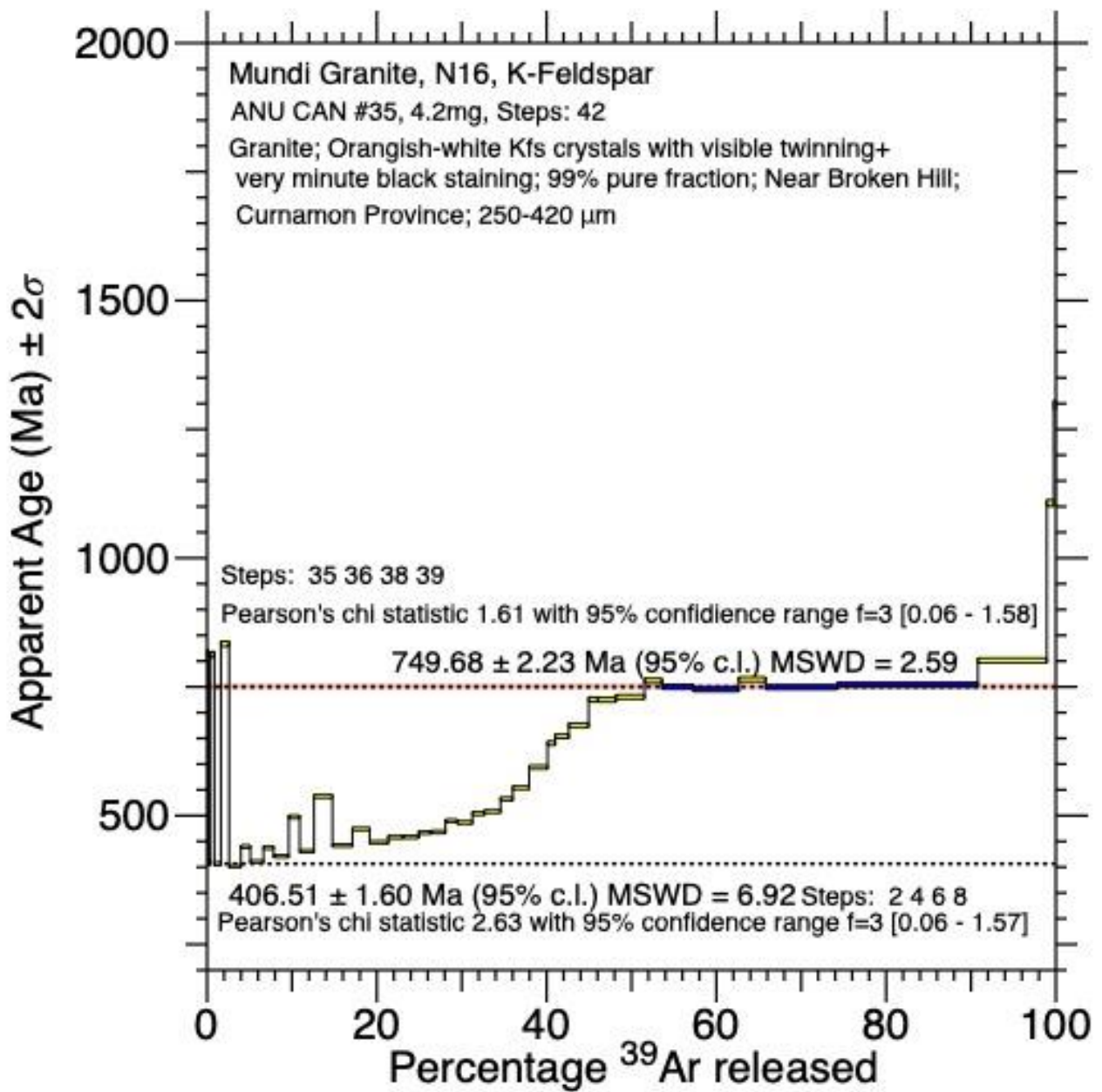


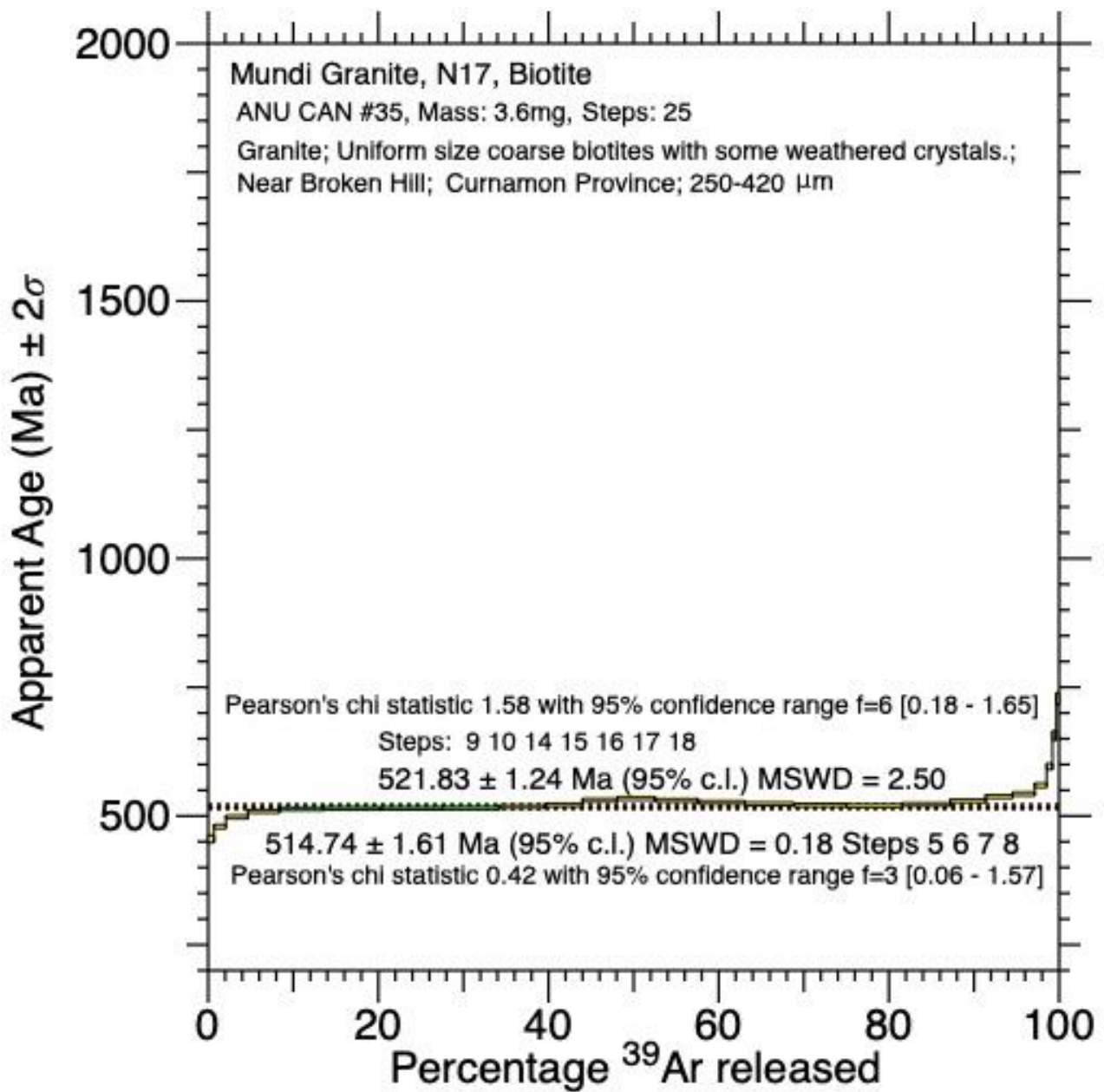










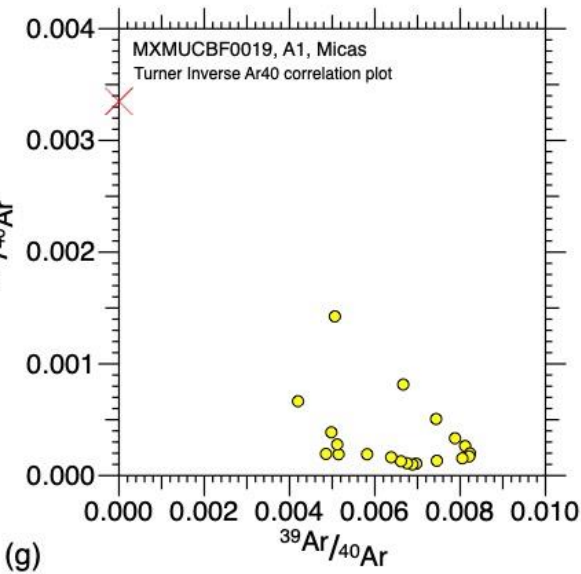
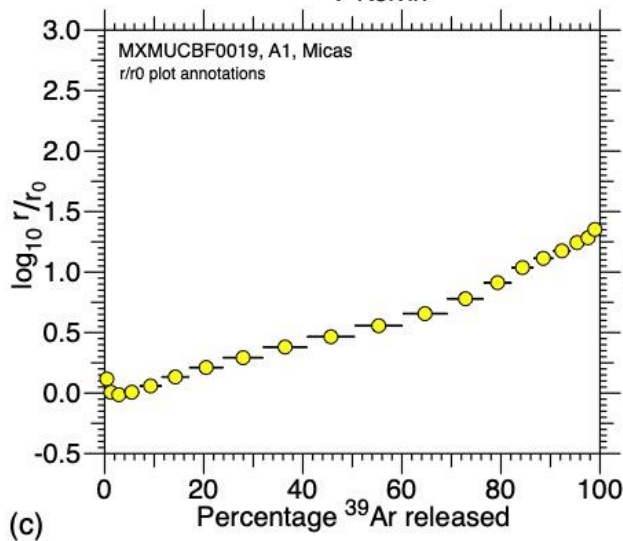
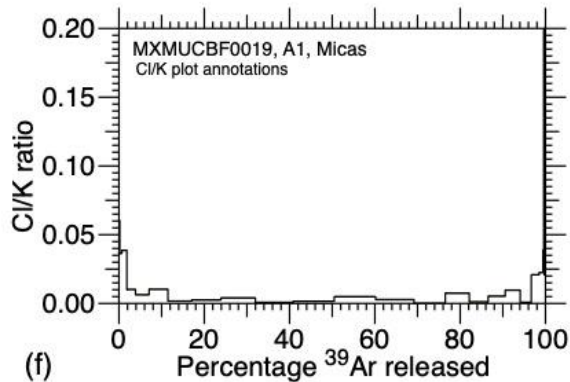
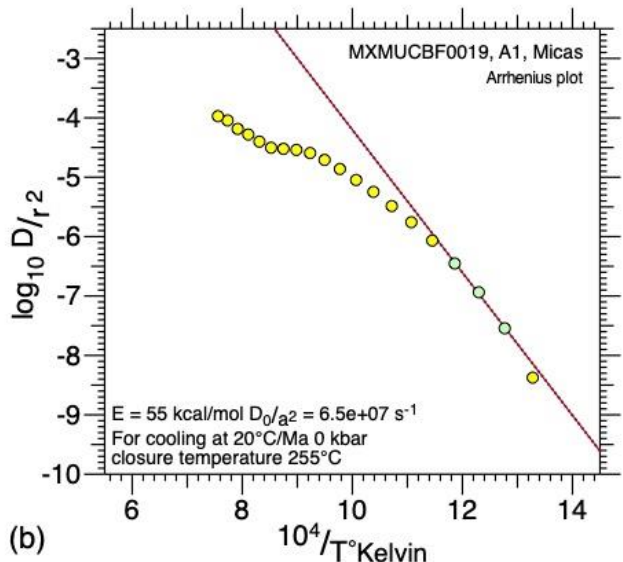
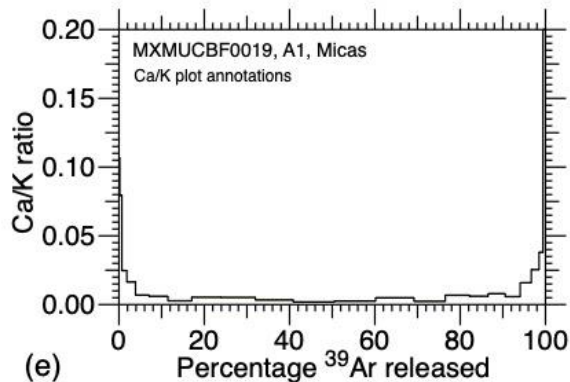
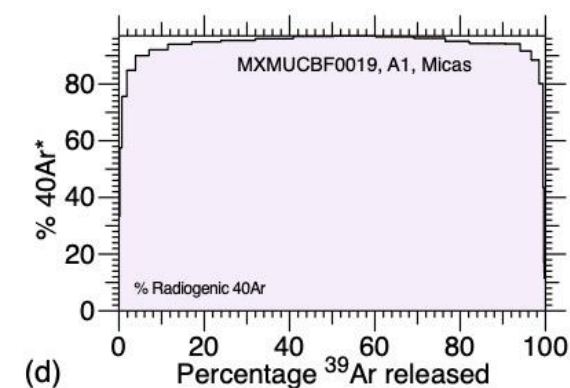
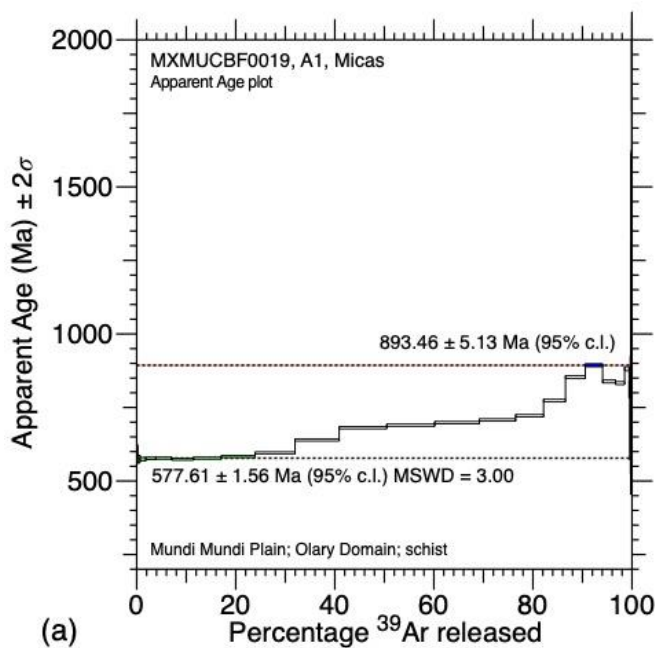


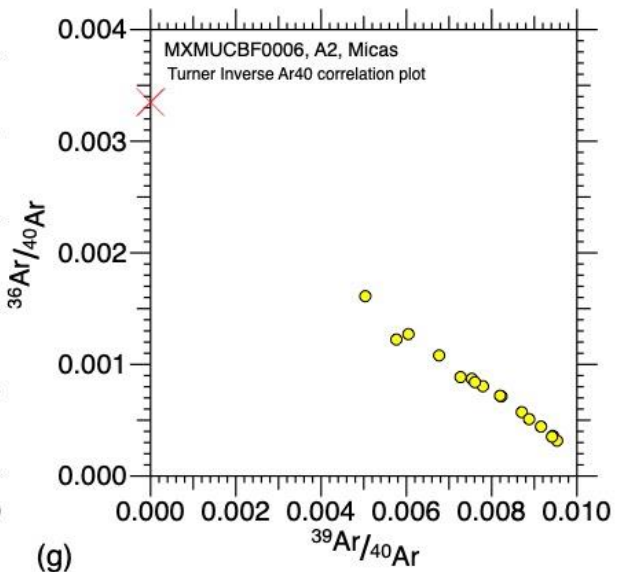
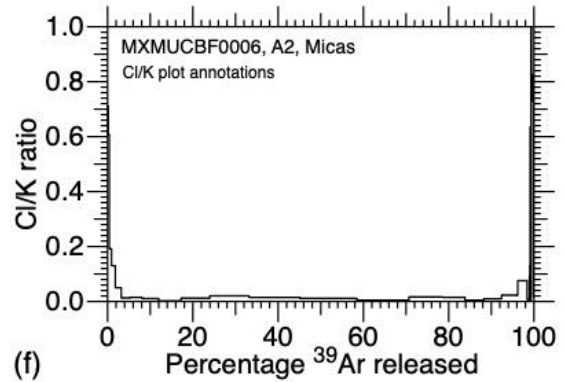
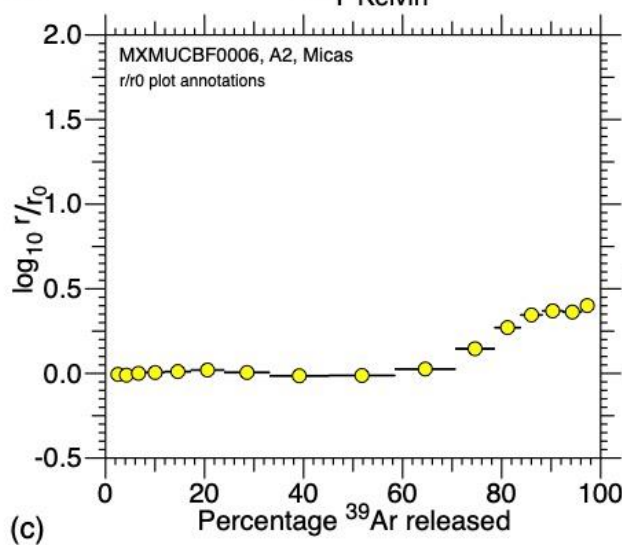
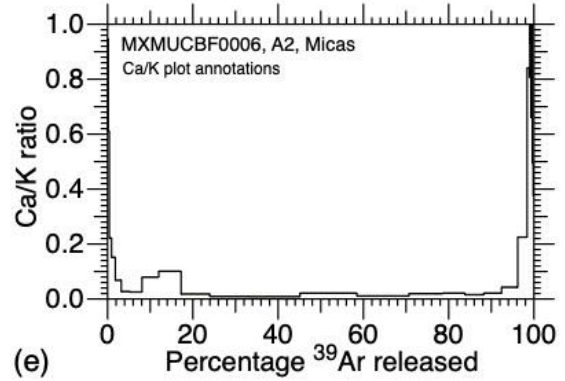
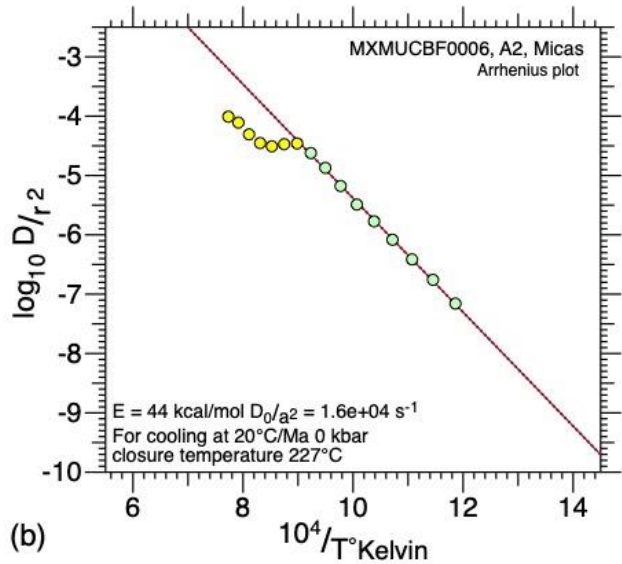
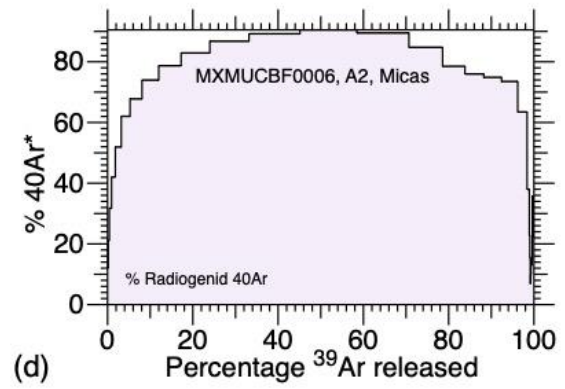
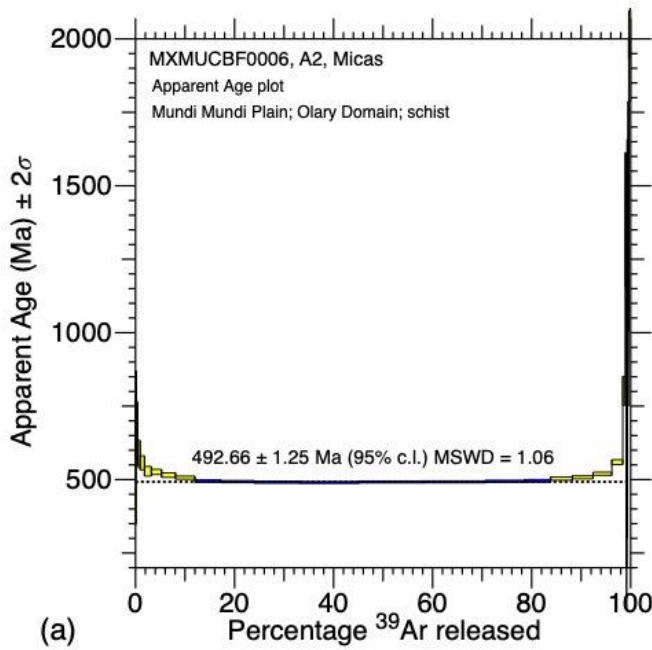
## Additional plots:

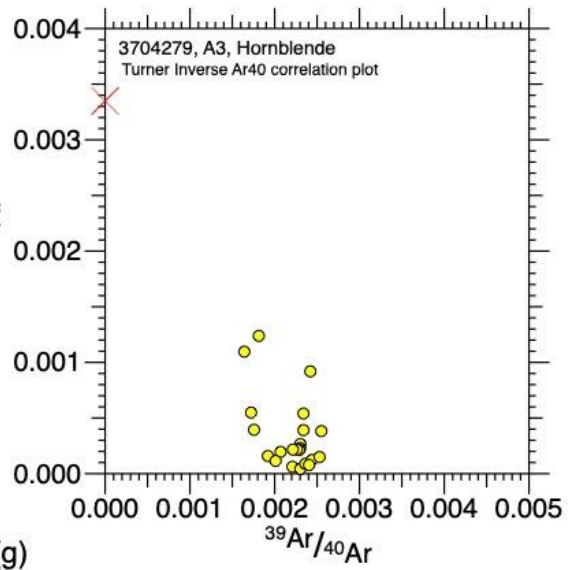
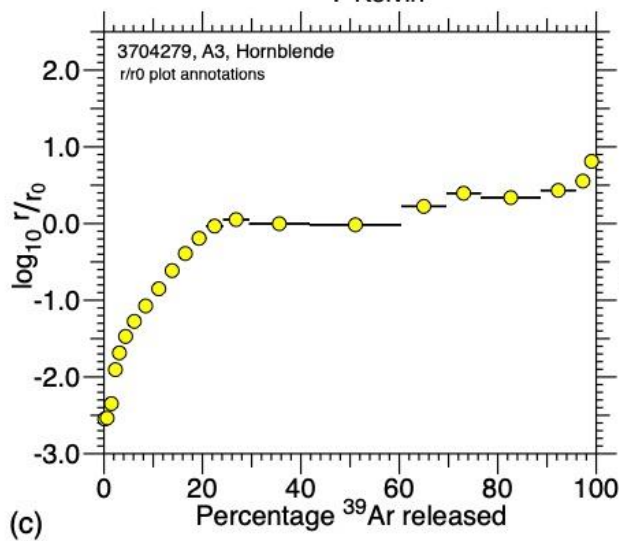
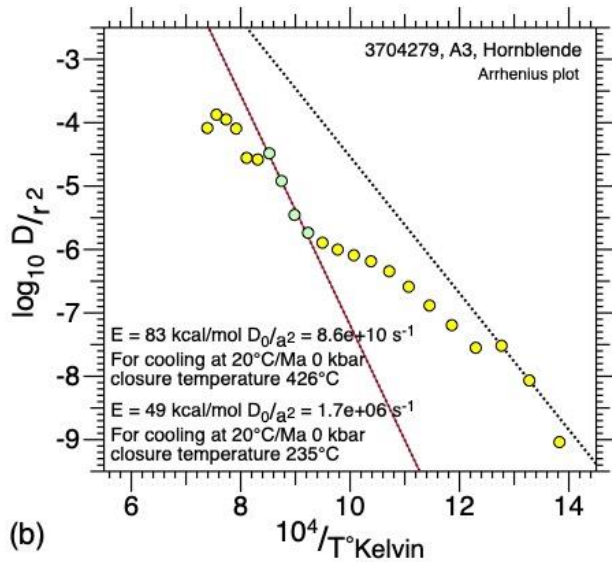
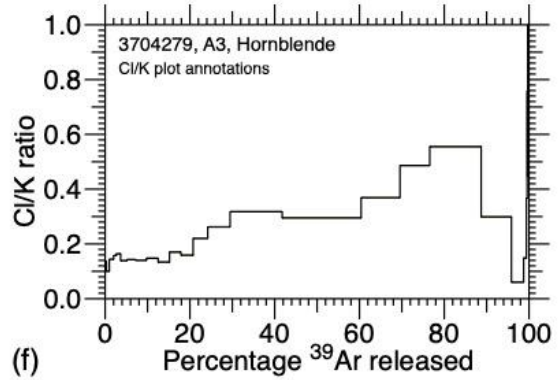
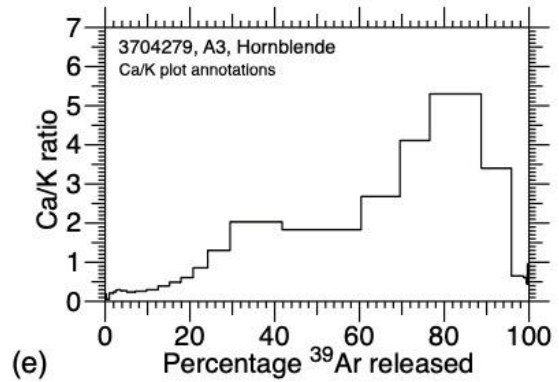
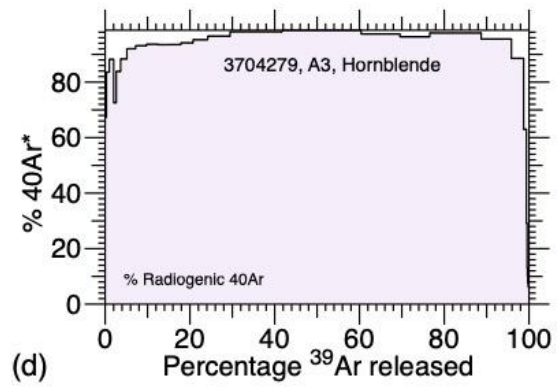
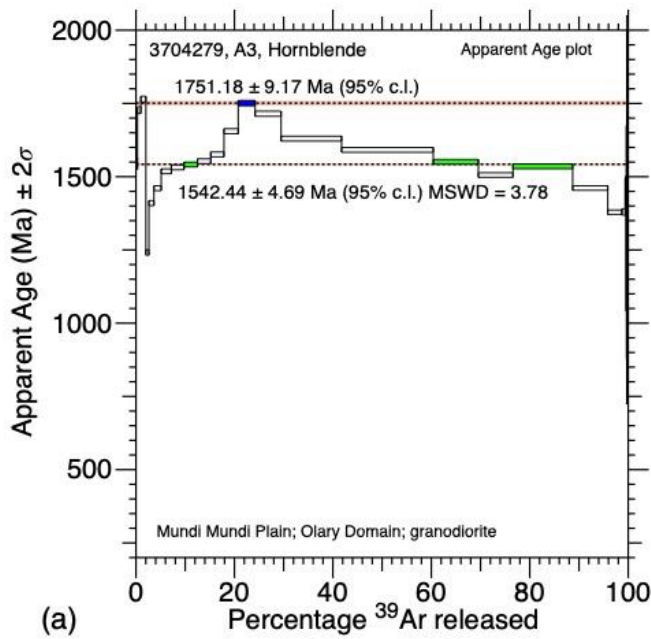
The following pages include nine different plots for each sample:

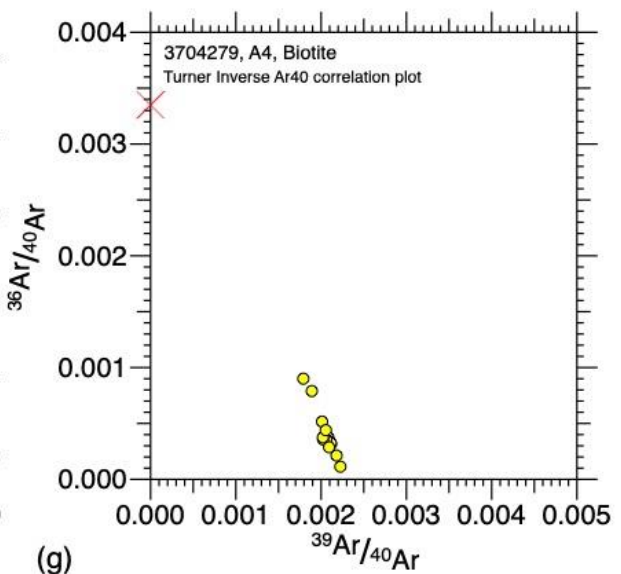
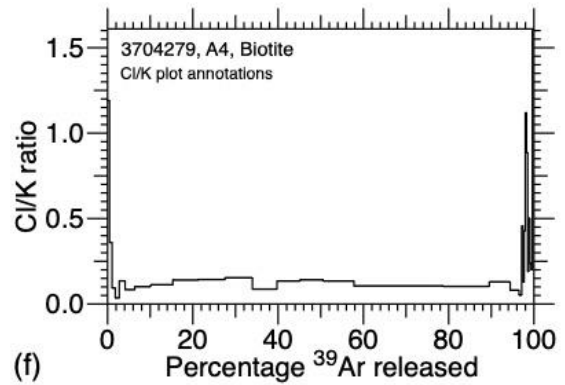
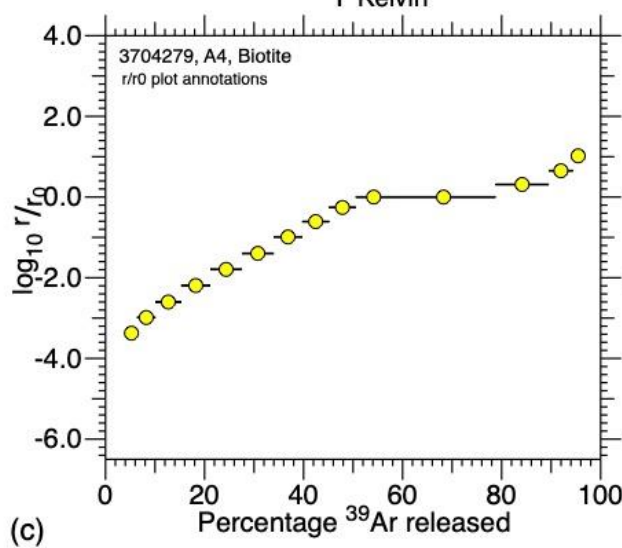
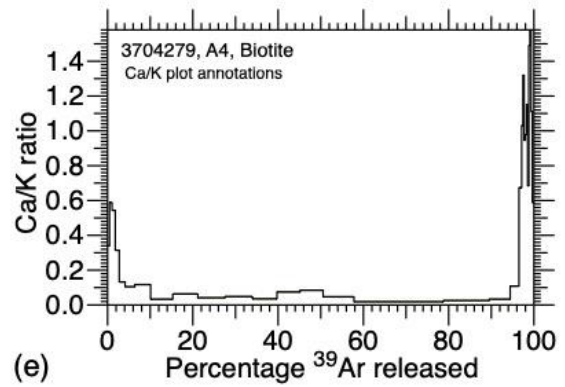
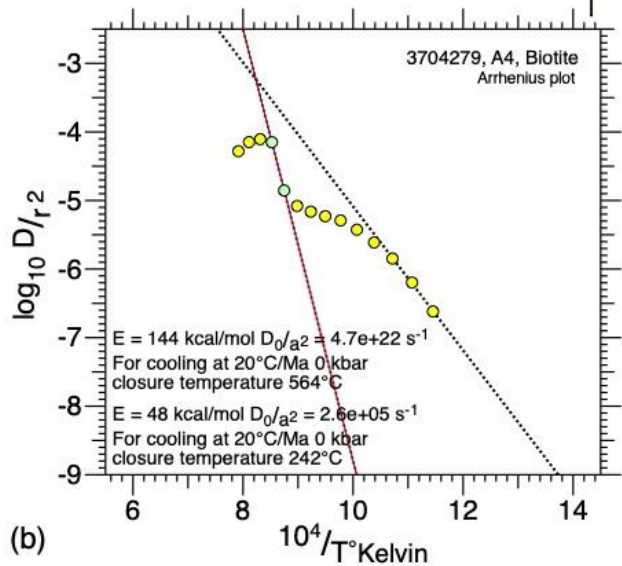
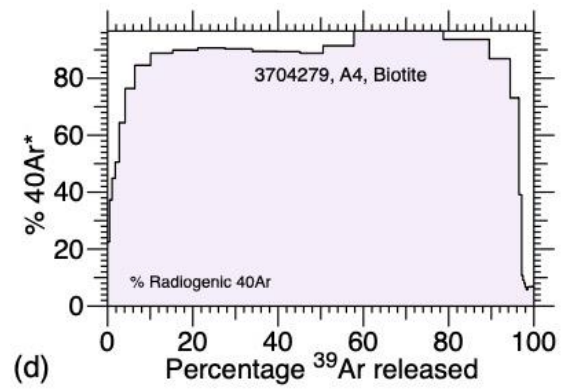
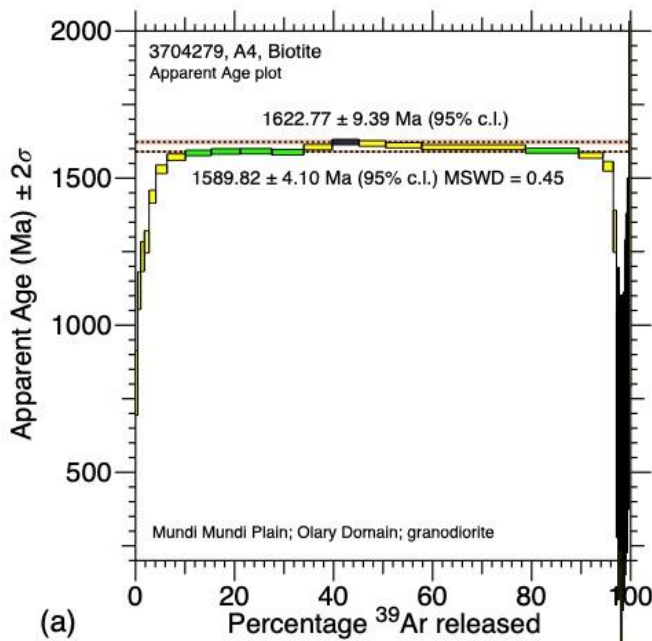
- Apparent Age Spectrum
- Arrhenius Plot (these are an estimate only).
- $r/r_0$  Plot
- Percentage Radiogenic Argon
- Ca/K Plot
- Cl/K Plot
- Turner Plot

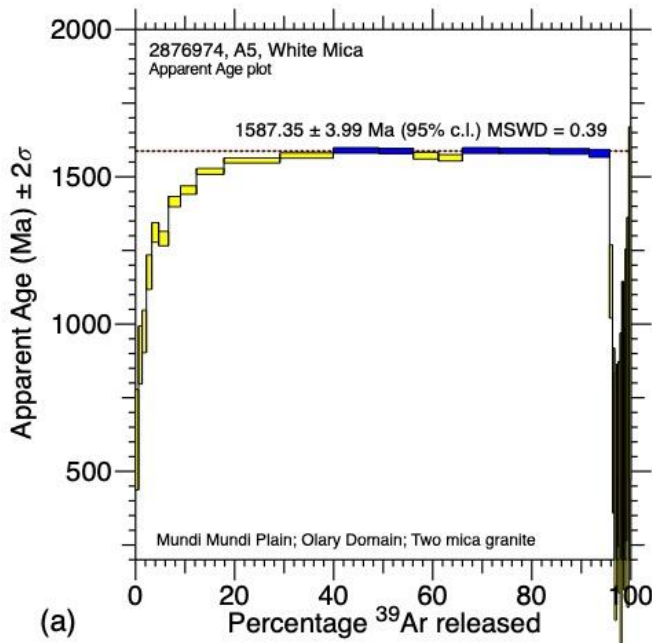
These are provided to enhance the understanding of the analytical results.



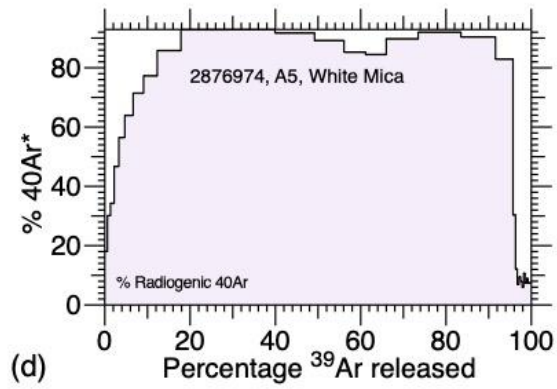




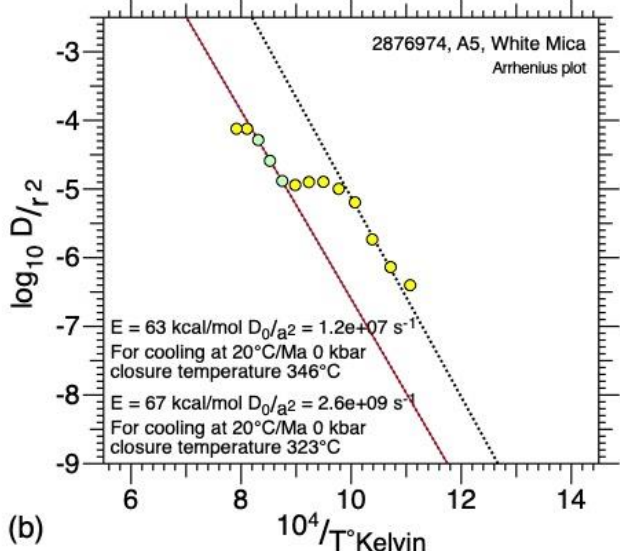




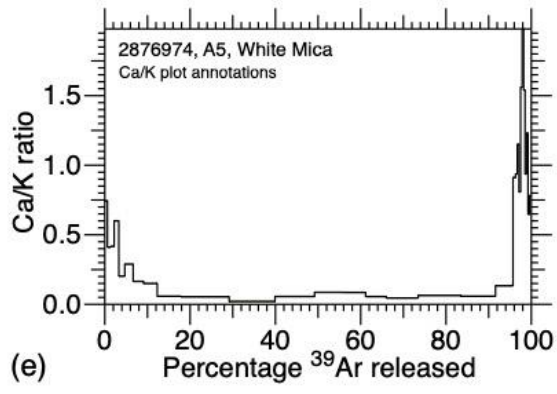
(a)



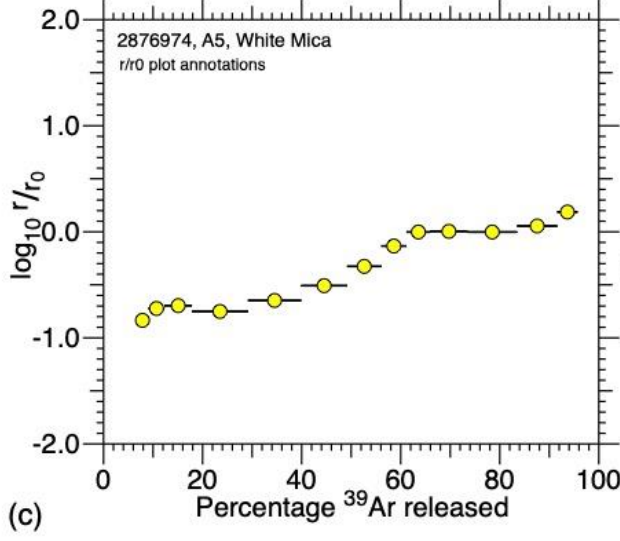
(d)



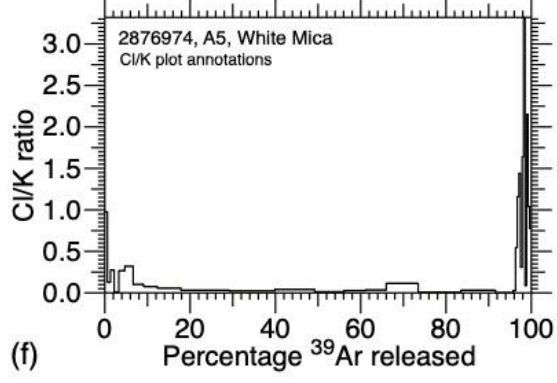
(b)



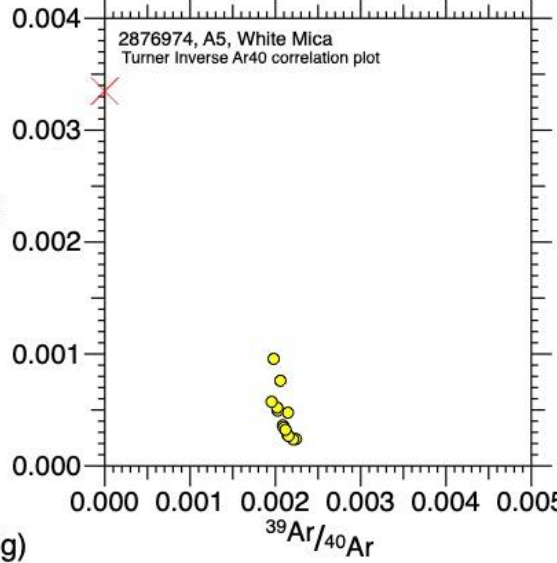
(e)



(c)

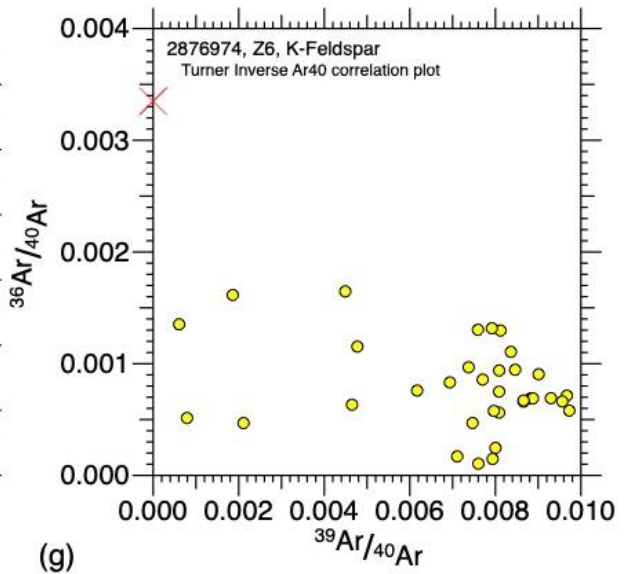
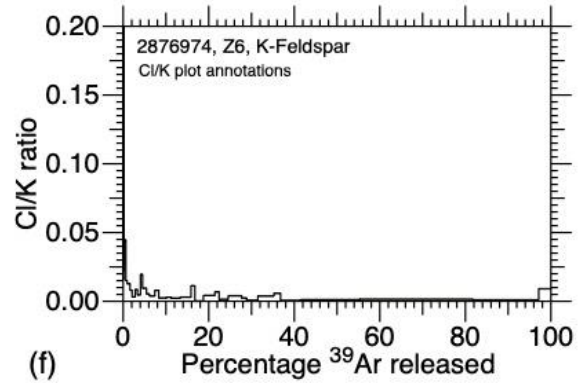
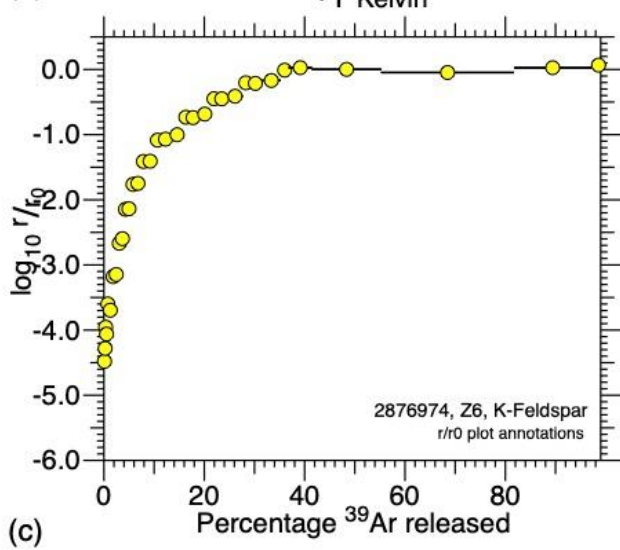
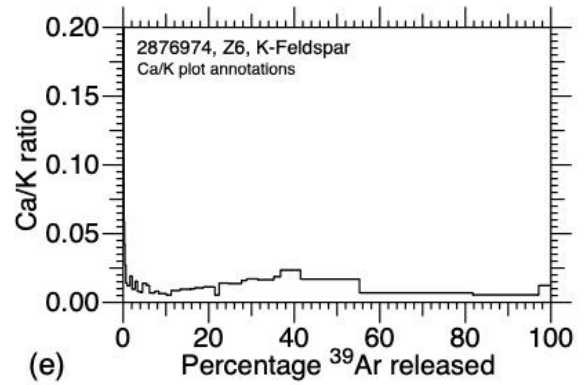
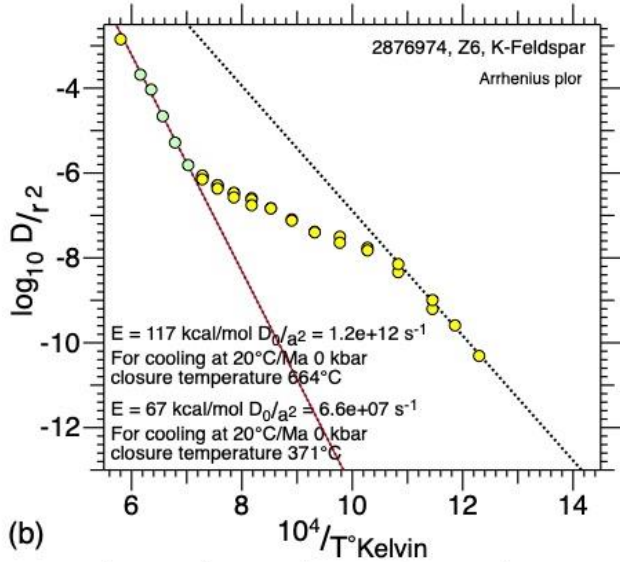
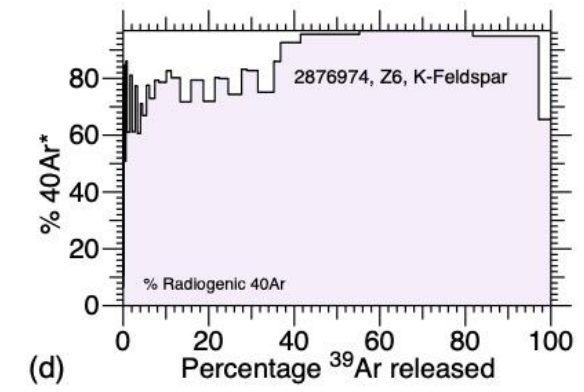
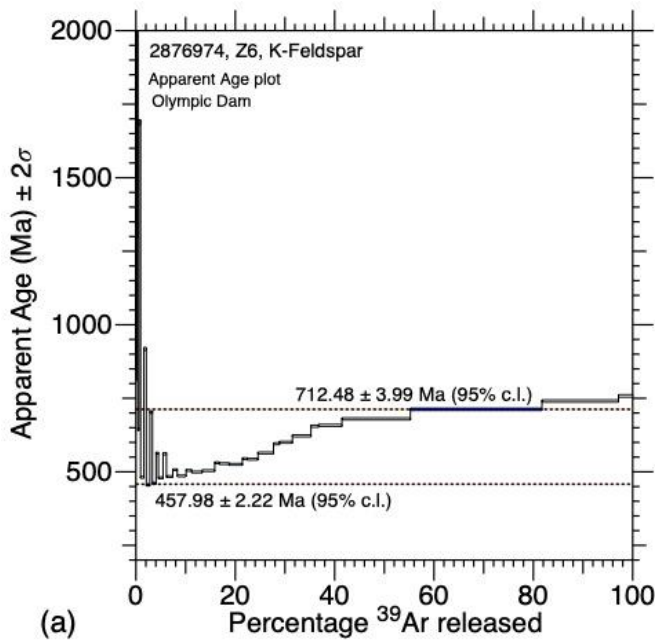


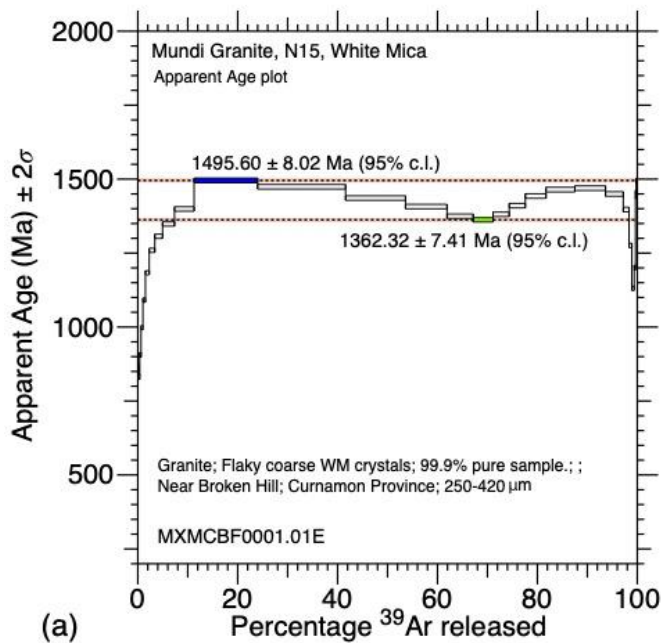
(f)



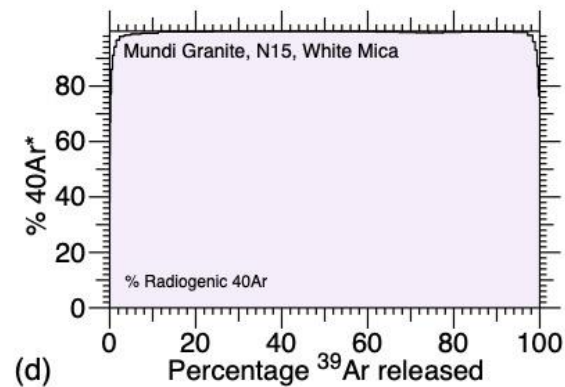
(g)



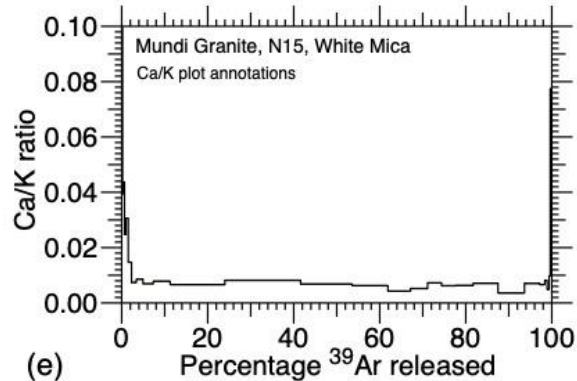




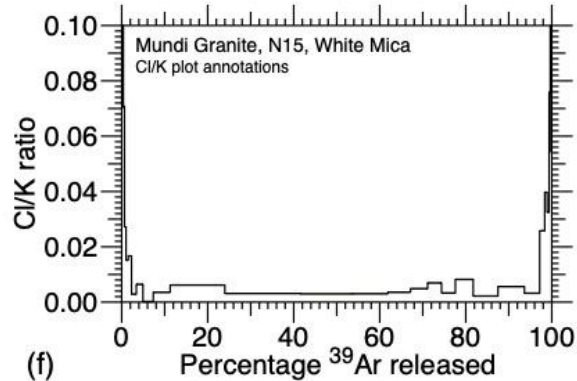
(a)



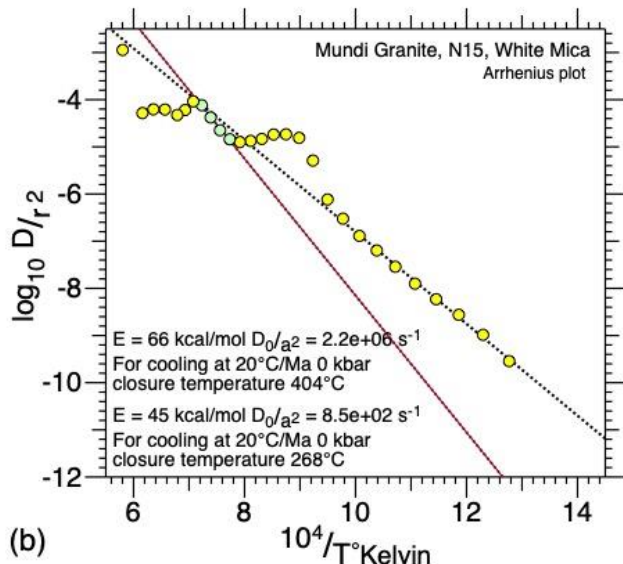
(d)



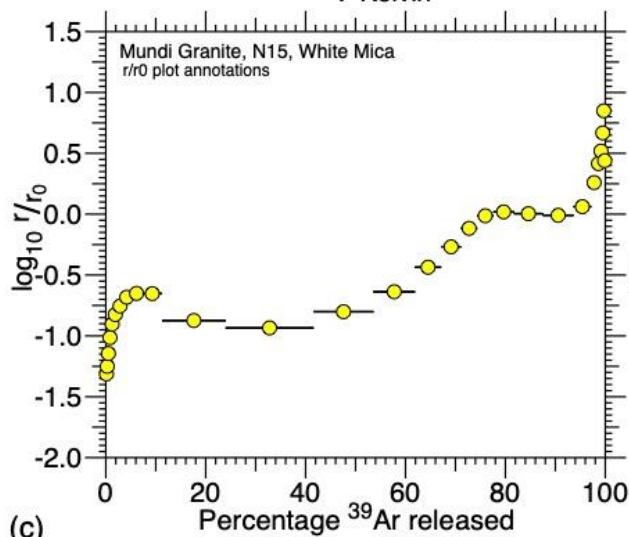
(e)



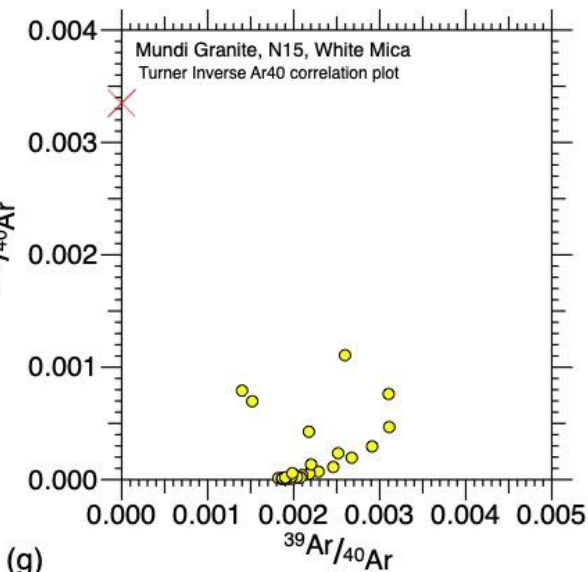
(f)



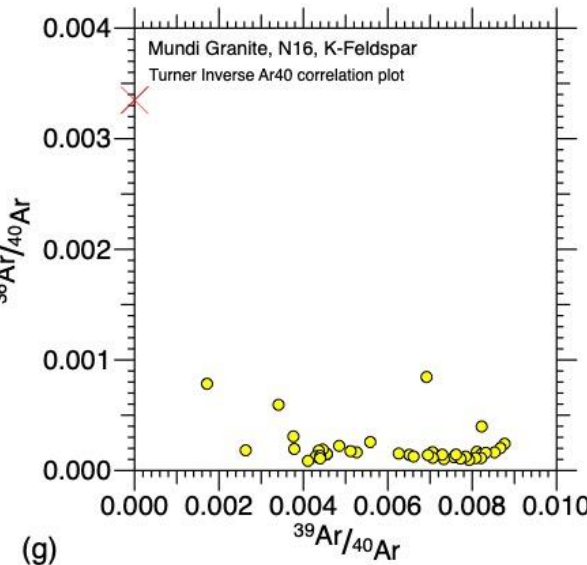
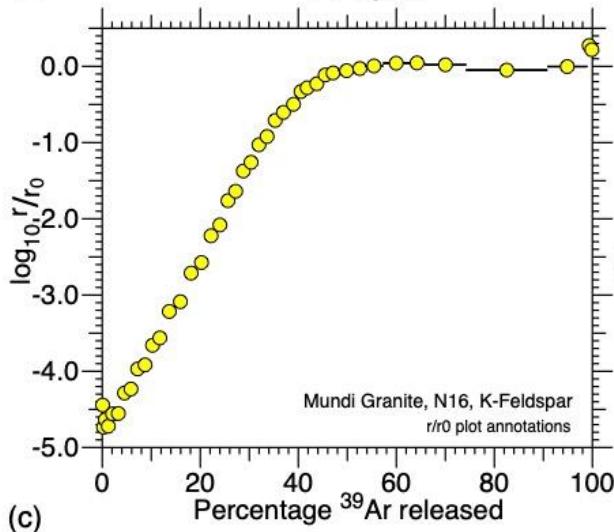
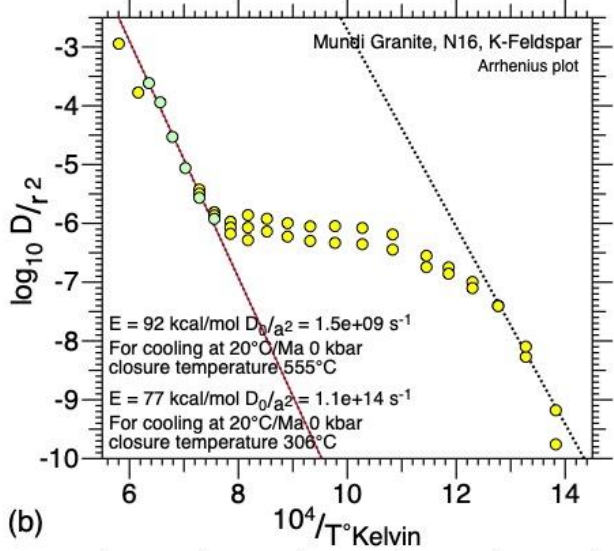
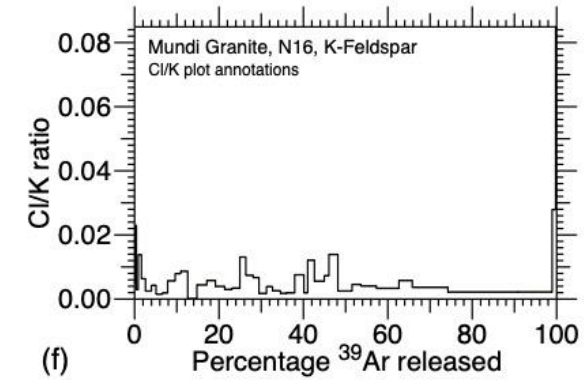
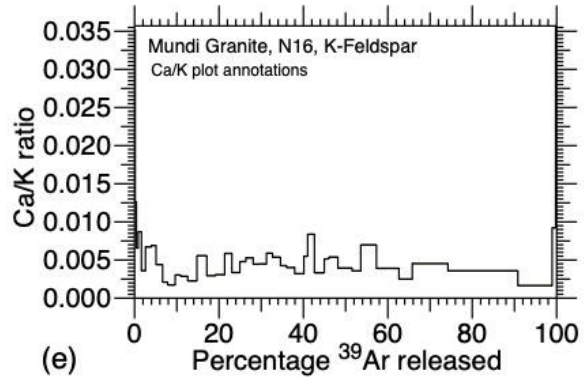
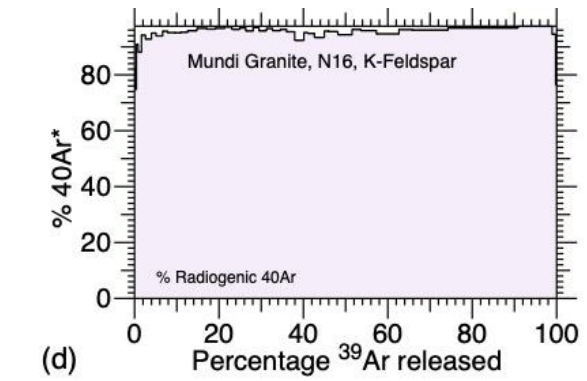
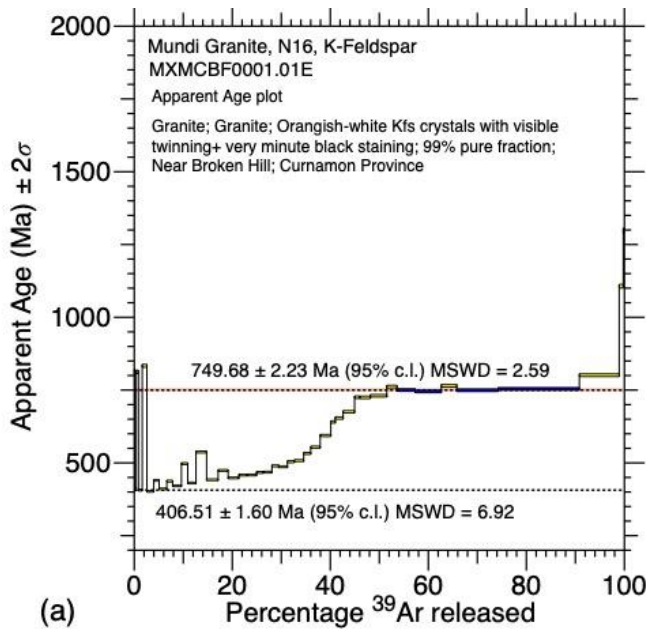
(b)

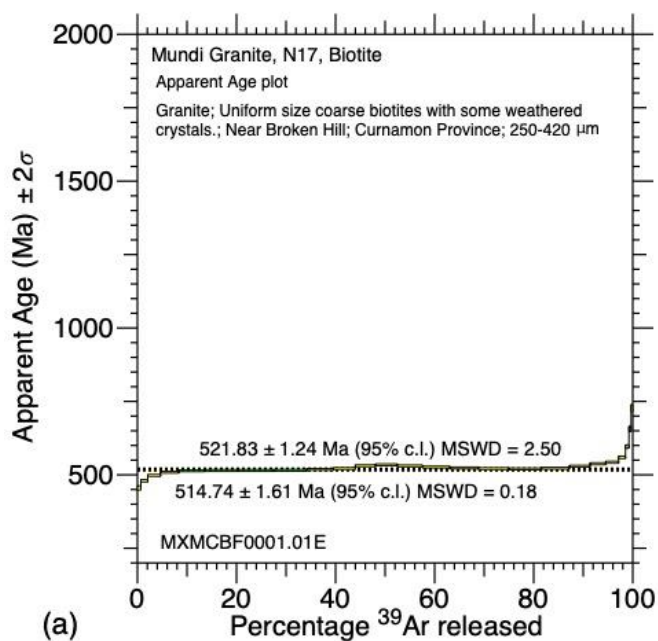


(c)

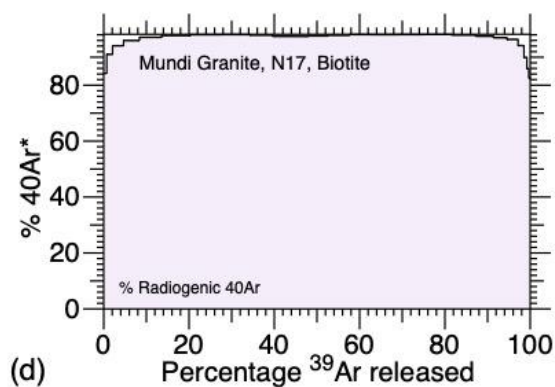


(g)

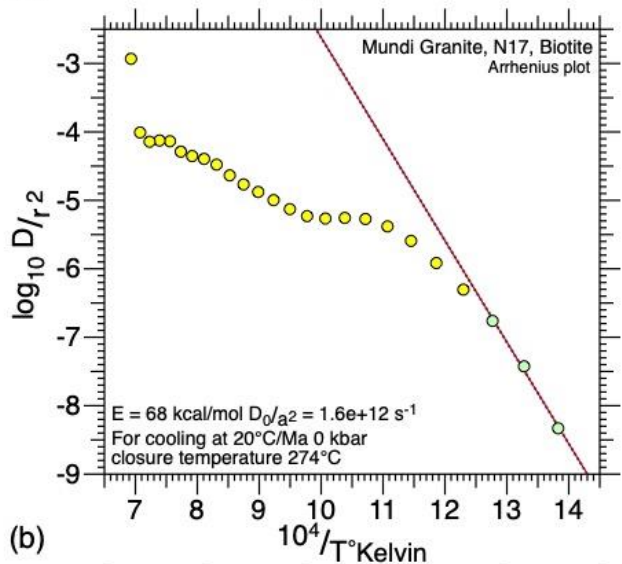




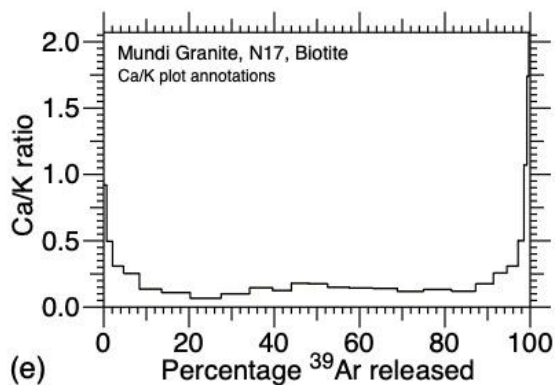
(a)



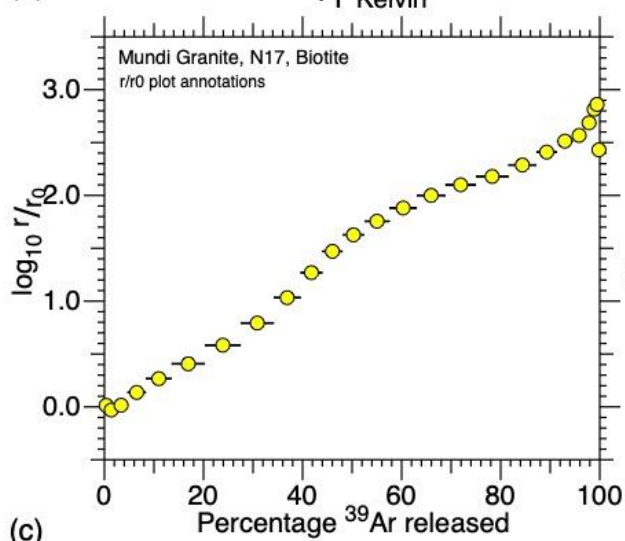
(d)



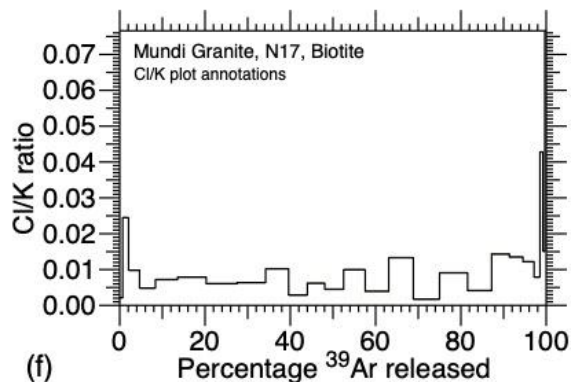
(b)



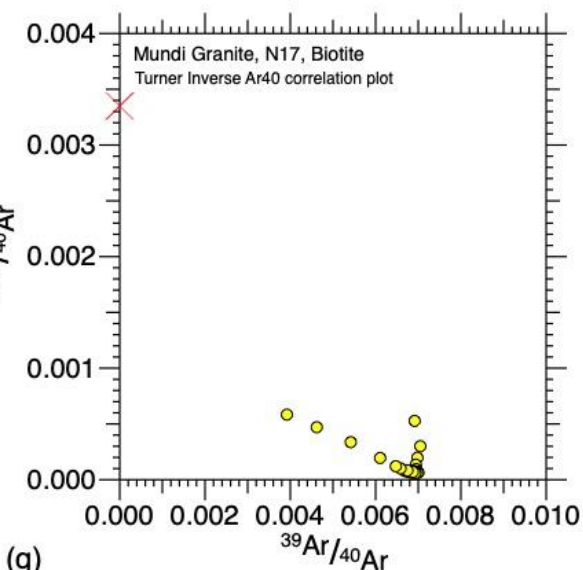
(e)



(c)



(f)



(g)

## **Supplementary Data:**

ANU Argon Facility Technical Report: ANU15-2021

40Ar/39Ar Analysis for National Argon Map

By Marnie Forster and Davood Vasegh

## **NAM Proposal 22:**

### **Ar-Ar thermochronology age constraints on mafic and felsic magmatism, and deformation in the Curnamona Province**

## **Methods and procedures**

### **Sample selection and mineral separation:**

The samples in this study were provided by Geological Survey of New South Wales and Geological Survey of South Australia. The separation procedures were undertaken in rock crushing and mineral separation laboratories at The Australian National University (Table 1). No chemical or leaching treatments were used during separation.

Mineral separation begins by choosing the most pristine sections with no evidence of weathering or staining. For samples with a targeted microstructure, the rock is first sliced into thin slabs using a trim saw, the selected area was then cut from the rock using a band saw. Once the selected area was separated, it was then crushed, milled and de-slimed as many times as was necessary to clean the grains and finally washed in deionised water.

### **K-feldspar procedure:**

For these minerals the grains are sieved into size fractions as recorded in Table 1 and passed through 0.25A then 1.0A current using a Frantz magnetic separator. K-feldspars are concentrated in the non-magnetic 1A fraction. This grain fraction is then separated under gravity using the Lithium heteropolytungstates (aq) (LST) heavy liquid at 2.58 g/cm<sup>3</sup>. K-feldspars are concentrated in the lighter than 2.58 g/cm<sup>3</sup> size fraction. The separated grains are washed as many times as was necessary to remove any residue LST on the grains with deionised water. Final hand-picking of the best quality grains was done in the Argon Preparation Laboratory.

### **Mica (Muscovite) procedure:**

For these minerals the grains are sieved into size fractions as recorded in Table 1, based on actual grain size in the sample. Additional white mica is obtained through 0.25A then 1.0A current using a Frantz magnetic separator. Final hand-picking of the best quality grains was done in the Argon Preparation Laboratory.

### **Biotite (Phlogopite) procedure:**

For these minerals the grains are sieved into size fractions as recorded in Table 1, based on actual grain size in the sample. Paper concentration is performed on the size fraction to obtain the purest mineral separation as possible. Additional biotite is obtained by separating grains through 0.25A current using a Frantz magnetic separator, with biotite concentrated in the magnetic 0.25A fraction. Final hand-picking of the best quality grains was done in the Argon Preparation Laboratory.

### **Hornblende procedure:**

For these minerals the grains are sieved into size fractions as recorded in Table 1 based and passed through 0.25A current using a Frantz magnetic separator. Hornblendes are concentrated in the magnetic 0.25A fraction. If the separates from FRANTZ is not pure (i.e.  $\geq 50\%$  hornblende), this grain fraction is then separated under gravity using the Lithium heteropolytungstates (aq) (LST) heavy liquid at 2.9 g/cm<sup>3</sup>. Hornblendes are concentrated in the heavier than 2.9 g/cm<sup>3</sup> size

fraction. The separated grains are washed as many times as was necessary to remove any residue LST on the grains with deionized water Final hand-picking of the best quality grains was done in the Argon Preparation Laboratory.

**Mineral separation details:**

Sample ID	Target Mineral	Mass (mg)	Grain Size (µm)	Treatment / Comment	Picture
MXMUCBF0019	Micas	3.1	250-355	Mixture of 2 white mica generations. Very little distinct grain (white mica flakes), mostly micaceous aggregates with a yellow-green hue and some black dots	
MXMUCBF0006	Micas	2.4	250-420	Grain separates, micaceous material	
3704279	Hornblende	83.6	250-420	Pristine grain, few dark, small inclusions	
3704279	Biotite	3.7	355-420	Potentially slight weathering. Thick, pristine biotite with gold tint	
2876974	Muscovite	3.5	355-420	Pristine white mica with similar grain size, slight green hue	

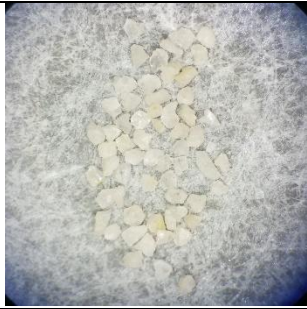
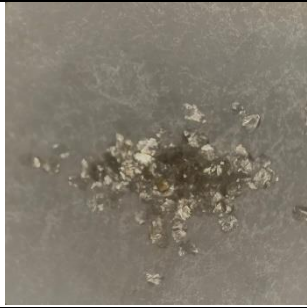


2876974	K-feldspar	4.4	355-420	Pristine grains with some yellow hue	
Mundi Mundi Granite	White mica	3.5	250-420	Flaky coarse WM crystals; 99.9% pure sample.	
Mundi Mundi Granite	K-Feldspar	4.2	250-420	Orangish-white Kfs crystals with visible twinning+ very minute black staining; 99% pure fraction	
Mundi Mundi Granite	Biotite	3.6	250-420	Uniform size coarse biotites with some weathered crystals.	

Table 1: Mineral separation details

### Sample irradiation details:

Irradiation of samples for  $^{40}\text{Ar}/^{39}\text{Ar}$  analysis was undertaken at the University of California Davis McClellan Nuclear Research Centre, CA, US in Central Facility position of TRIGA reactor without rotation, with 1.0mm of Cadmium shielding in different batches as listed below:

- **ANU CAN #35** => 12.00 hours (19-20 Dec 2019)
- **ANU CAN #38** => 18.00 hours (23-25 Jun 2021)
- **ANU CAN #39** => 20.00 hours (25-28 Oct 2021)

The calculated amounts of grains were weighed and recorded and then wrapped in labelled aluminium packets in preparation for irradiation. The sample filled foils were placed into a quartz irradiation canister together with aliquots of the flux monitor Biotite GA1550. The foil packets of GA1550 standards were dispersed 6-8mm apart throughout the irradiation canister, between the unknown age samples. In addition, packets containing  $\text{K}_2\text{SO}_4$  and  $\text{CaF}_2$  were placed in the middle of the canister to monitor argon isotope production from potassium and other interfering elements.

Irradiated samples were unwrapped upon their return to the Australian National University, and then rewrapped in tin foils in preparation for analysis under vacuum in the furnace. Tin foil is used because the melting temperature of tin is lower than the experiment starting point in the furnace and gasses from tin can be pumped away prior to the sample analysis.

## **$^{40}\text{Ar}/^{39}\text{Ar}$ procedures and analysis information**

### **Methodology:**

Temperature-controlled resistance furnace step-heating experiments is the technique that is used in the ANU Argon laboratory to extract argon isotopes from the samples to ensure 100% release of  $^{39}\text{Ar}$ . A sample is dropped into a cleaned furnace and heated to 400°C to melt the tin foil and then left in the furnace at 350°C for 8-12 hours to pump away unwanted gases. This cleaning procedure has proven to significantly improve the quality of the resultant data. The step-heating experiment then starts at 450°C, and each incremental heating step is heated at a constant temperature for 15 minutes. The heating process involves rapid heating to the setpoint temperature with no overshoot, then temperature is maintained for 15 minutes followed by rapid cooling; this procedure produces a square wave in temperature for each heating step. The heating step schedule for biotite and muscovite rises by 30°C increments (except for the last a few steps), with 30 steps per sample, while K-feldspar is analysed in more than 40 steps, including numerous isothermal steps. Diffusion experiments, as conducted in the ANU Argon laboratory, are designed to retrieve diffusion parameters which can be used in quantitative temperature-time modelling. The heating schedules are recorded in the Excel Tables for each sample.

Cleaning of the furnace between samples is vital in this method. The furnace is degassed four times at 1,450°C for 15 minutes and the gas pumped away prior to the loading of the subsequent sample. Blanks are measured to monitor the cleaning process. The flux monitor crystals are fused using a  $\text{CO}_2$  continuous-wave laser. Gas released from either the flux monitors or each step of the sample analyses are exposed to three Zr-Al getters; two AP10 (Cold and hot) and one CP50, each for 10 minutes, to remove active gases. The purified extracted gasses are then isotopically analysed in the Argus VI mass spectrometer. The  $^{40}\text{Ar}/^{39}\text{Ar}$  dating technique is adapted from McDougall and Harrison (1999) and described in Forster and Lister (2009).

Background levels are measured and subtracted from all analyses, from flux monitors and samples. The nuclear interfering values for the correction factors for the isotopes are listed below (Tetley et al 1980). These are measured for the reactions and uncertainties of  $(^{36}\text{Ar}/^{37}\text{Ar})_{\text{Ca}}$ ,  $(^{39}\text{Ar}/^{37}\text{Ar})_{\text{Ca}}$ ,  $(^{40}\text{Ar}/^{39}\text{Ar})_{\text{K}}$ ,  $(^{38}\text{Ar}/^{39}\text{Ar})_{\text{K}}$  and  $(^{38}\text{Ar})_{\text{Cl}}/(^{39}\text{Ar})_{\text{K}}$ , and were calculated prior to sample analyses.

### **Mass spectrometer setup and procedures**

Samples and standards were analysed in the Argon Laboratory at the Research School of Earth Science, The Australian National University, Canberra, Australia using a *Thermo Fisher ARGUS-VI* multi-collector mass spectrometer (Table 2).

Mass Spectrometer:	Thermo Fisher Argus VI
Detector Type:	Faraday Cups only x5
Calibrations:	3 levels (Zero Offset, Gain and Cross Calibration)
Peak Centring:	Once for every measurement @H2 ( $^{40}\text{Ar}$ )
Measurement Cycles:	51 cycles on all detectors
Extrapolation Method:	Exponential extrapolation and uncertainty



Name	UFC Offset [fA]	Gain	Cross Calibration Factor
H2	-4.9761469	0.9871203	1
H1	-2.2071069	0.9671459	1.007184188
AX	-7.6814703	0.9769602	1.017518151
L1	-2.3979322	0.9706487	1.030604297
L2	-3.1329948	0.9676338	1.047244337

Table 2: Detector Calibration Values

**The calculation parameters:**

Lambda <sup>40</sup> K (Renne et al 2011)	5.5305E-10
Lambda <sup>37</sup> Ar (Kondev et al 2017)	1.9798E-02
Lambda <sup>39</sup> Ar (Kondev et al 2017)	7.0548E-06
Lambda <sup>36</sup> Cl (Kondev et al 2017)	6.2985E-09
Ca/K conversion factor	1.90
Flux Monitor	GA1550 @ 99.18 ± 0.14 Ma

**Atmospheric Argon correction ratio:**

<sup>40</sup> Ar/ <sup>36</sup> Ar (Lee et al 2006)	298.57
<sup>40</sup> Ar/ <sup>38</sup> Ar (Lee et al 2006)	1,583.52

**Interfering isotope production ratios:**

Correction Factor	CAN #35	CAN #38	CAN #39
( <sup>36</sup> Ar/ <sup>37</sup> Ar) <sub>Ca</sub>	2.32216E-04	1.96095E-04	1.79735E-04
( <sup>39</sup> Ar/ <sup>37</sup> Ar) <sub>Ca</sub>	6.16219E-04	8.53577E-04	1.12340E-03
( <sup>40</sup> Ar/ <sup>39</sup> Ar) <sub>K</sub>	2.46117E-02	2.68686E-02	4.07978E-02
( <sup>38</sup> Ar/ <sup>39</sup> Ar) <sub>K</sub>	1.16607E-02	1.15556E-02	1.15626E-02
( <sup>38</sup> Ar) <sub>Cl</sub> / <sub>(<sup>39</sup>Ar)<sub>K</sub></sub>	8.02854E-02	8.04746E-02	8.02810E-02

Table 3: Isotopes Interferences

**Representative air shot and blanks measurements:**

The discrimination factor was calculated by analysing five air shots on either side of sample analyses and is reported at 1amu. Table 4 shows an example of the analysed air shots and resultant calculation of discrimination factor.

Date	<sup>40</sup> Ar ± %err		<sup>38</sup> Ar ± %err		<sup>36</sup> Ar ± %err		1amu ± %err		Reported Value 1.0014890 ± 0.107%
14-Sep-2021	1,967.110	0.011	1.237	1.536	6.632	0.266	1.00166	0.143	
14-Sep-2021	1,963.428	0.011	1.239	1.593	6.618	0.295	1.00160	0.156	
14-Sep-2021	1,966.338	0.010	1.252	1.335	6.613	0.255	1.00105	0.138	
14-Sep-2021	1,962.069	0.011	1.267	1.337	6.636	0.316	1.00244	0.166	
14-Sep-2021	1,964.723	0.011	1.270	1.502	6.599	0.255	1.00070	0.138	

Table 4: Air Shots and Mass Discrimination Factor

The blank measurements are undertaken with different temperature schedules between 300°C and 1450°C, depending on the degassing behaviour and previous blank measurement results. The degassing and blank measurement procedure continues until the ratios of <sup>40</sup>Ar, <sup>38</sup>Ar and <sup>36</sup>Ar drop to atmospheric ratios, and <sup>39</sup>Ar and <sup>37</sup>Ar drop below detectable levels. The entire procedure of degassing and blank measurements is repeated at the end of a set of samples. Blanks will be done in-between samples that belong to a set, with reduced steps at 300°C, 1300°C and 1450°C to check

isotope levels. In addition, the mass of each sample is calculated so that the volume of gas released from each step overwhelms the volume of gas that may occur in the blank. The table 5 is a representative sequence of measured blank values recorded during a monitoring process.

Temperature	<sup>40</sup> Ar	<sup>39</sup> Ar	<sup>38</sup> Ar	<sup>37</sup> Ar	<sup>36</sup> Ar	<sup>40</sup> Ar/ <sup>36</sup> Ar
300	1817.738	0.708661	1.209615	ND*	6.113996	297.3077
500	1879.391	0.741332	1.266375	ND	6.364901	295.2743
700	1911.306	0.759696	1.282523	0.095807	6.417252	297.8386
900	2053.27	0.775687	1.358664	ND	6.94095	295.8198
1100	2731.788	0.812587	1.788944	0.10454	9.192207	297.1852
1300	7305.089	1.038774	4.728446	0.139915	24.59727	296.9878
1450	36811.09	2.436249	23.78145	0.23653	124.4077	295.8909
300	748.5261	0.344558	0.467985	0.019884	2.5069	298.5864
1300	1126.281	0.438838	0.704102	0.0207706	3.744338	300.7958
1450	2181.428	1.00614	1.377076	0.1028531	7.299197	298.8587

Table 5: Example of the blanks measurements during a sequence of blanks where isotopes were being monitored prior to sample analysis (\* => Not Detectable). Temperature is °C.

#### Data reduction software:

The calculations were done with an adapted version of *Noble* Software (2020, developed and adapted by the Australian National University Argon Laboratory) and all interpretations have been undertaken with *eArgon* (developed and adapted for ANU Argon Laboratory by G.S. Lister).

#### Reported Data:

The reported data have been corrected for system backgrounds, mass discrimination, fluence gradients and atmospheric contamination. GA1550 standards were analysed, and an exponential best fit was then used for the calculation of the J-factor and J-factor uncertainty (Table 6).

#### Samples J-Factor, Mass Discrimination, and uncertainties:

Sample Name	Irradiation Batch	J-Factor ± %uncertainty		Mass Discrimination ± %uncertainty		Measurement Date
MXMUCBF0019	#38	3.29289E-03	0.1851	1.00164	0.119	10-Sep-2021
MXMUCBF0006	#38	3.29273E-03	0.1851	1.00149	0.107	12-Sep-2021
3704279	#38	3.29257E-03	0.1851	1.00149	0.107	15-Sep-2021
3704279	#38	3.29241E-03	0.1851	1.00149	0.107	17-Sep-2021
2876974	#38	3.29225E-03	0.1851	1.00115	0.102	19-Sep-2021
2876974	#39	3.79091E-03	0.1713	1.00524	0.103	07-Feb-2022
Mundi Mundi Granite (WM)	#35	2.35201E-03	0.2317	1.00417	0.095	06-May-2020
Mundi Mundi Granite (Kfs)	#35	2.35183E-03	0.2317	1.00407	0.102	04-May-2020
Mundi Mundi Granite (Bt)	#35	2.35164E-03	0.2317	1.00180	0.087	25-Aug-2020

Table 6: Sample analysis and calculation details

<sup>40</sup>Ar/<sup>39</sup>Ar isotopic data of the samples are supplied in the Excel Data Tables, which include details on the heating schedule, Argon isotopes abundances and their uncertainty levels, %Ar\*, <sup>40</sup>Ar\*/<sup>39</sup>Ar(K), Cumulative <sup>39</sup>Ar%, calculated age and its uncertainty, Ca/K, Cl/K, J-Factor and its uncertainty. Noting that all the reported uncertainties are at one sigma level and the fractional uncertainties are shown

as % in the headings of the appropriate columns of data tables. The components involved in the calculation of the uncertainties are listed in Table 7.

Uncertainty of:	Components involved in the calculation
Isotope Abundances	Uncertainty of isotope measurement Uncertainty of Mass Discrimination Factor (except for $^{39}\text{Ar}$ )
J-Factor	Uncertainty of $^{40}\text{K}$ Decay Constant Uncertainty of Age of the Flux monitor Uncertainty of Flux monitor isotopes abundances
Calculated Age	Uncertainty of Isotopes Abundances J-Factor value and uncertainty of J-Factor $^{40}\text{K}$ Decay Constant value and uncertainty of $^{40}\text{K}$ Decay Constant

Table 7: Components involved in the calculation of each uncertainty

### References:

- Forster, M.A. and Lister, G.S. 2004. The interpretation of  $^{40}\text{Ar}/^{39}\text{Ar}$  apparent age spectra produced by mixing: application of the method of asymptotes and limits. *Journal of Structural Geology* 26, 287–305
- Forster, M.A. and Lister, G.S. 2009. Core-complex-related extension of the Aegean lithosphere initiated at the Eocene-Oligocene transition. *Journal Geophysical Research*, 114, B02401.
- Kondev, F.G. and Naimi, S. 2017. The NUBASE2016 evaluation of nuclear properties. *Chinese physics C*, 41(3), p.030001.
- Lee, J.Y., Marti, K., Severinghaus, J.P., Kawamura, K., Yoo, H.S., Lee, J.B. and Kim, J.S. 2006. A redetermination of the isotopic abundances of atmospheric Ar. *Geochimica et Cosmochimica Acta*, 70(17), 4507-4512.
- McDougall, I. and Harrison, T.M. (Eds.). 1999. *Geochronology and Thermochronology by the  $^{40}\text{Ar}/^{39}\text{Ar}$  Method*, 2nd ed., 269 pp. Oxford Univ. Press, New York.
- Renne, P.R., Balco, G., Ludwig, K.R., Mundil, R. and Min, K., 2011. Response to the comment by WH Schwarz et al. on “Joint determination of  $^{40}\text{K}$  decay constants and  $^{40}\text{Ar}^*/^{40}\text{K}$  for the Fish Canyon sanidine standard, and improved accuracy for  $^{40}\text{Ar}/^{39}\text{Ar}$  geochronology” by PR Renne et al.(2010). *Geochimica et Cosmochimica Acta*, 75(17), pp.5097-5100.
- Spell, T. L. and I. McDougall. 2003. Characterization and calibration of  $^{40}\text{Ar}/^{39}\text{Ar}$  dating standards. *Chemical Geology*, 198, 189–211.
- Tetley, N., McDougall, I. & Heydegger, H.R. 1980. Thermal neutron interferences in the  $^{40}\text{Ar}/^{39}\text{Ar}$  dating technique. *Journal Geophysical Research*, 85, 7201–7205.